Table 2 Sensitivity and specificity of cardiac ^{123}I-MIBG scintigraphy in differentiating Parkinson's disease from other parkinsonian syndromes

Total PD patients (n=24)												
	Early image						Delayed image					
Cut-off	1.80	1.85	1.90	1.95	2.00	2.05	1.60	1.65	1.70	1.75	1.80	1.85
Sensitivity	70.8%	75.0%	75.0%	79.2%	79.2%	79.2%	70.8%	75.0%	79.2%	79.2%	79.2%	87.5%
Specificity	93.3%	93.3%	93.3%	93.3%	86.7%	80.0%	93.3%	80.0%	73.3%	73.3%	73.3%	73.3%
Hoehn and Yahr 1 and 2 (n=15)												
	Early image						Delayed image					
Cut-off	1.80	1.85	1.90	1.95	2.00	2.05	1.60	1.65	1.70	1.75	1.80	1.85
Sensitivity	53.8%	61.5%	61.5%	69.2%	69.2%	69.2%	53.8%	61.5%	69.2%	69.2%	69.2%	84.6%

Cut-off levels, for which both the sensitivity and specificity were more than 70%, are shown. The optimal cut-off levels determined by receiver-operating characteristic analysis were at 1.95 and 1.60 in the early and delayed images, respectively

dopaminergic function assessed by ^{11}C-CFT uptake and disease stage determined according to the HY scale.

It has been reported that cardiac ^{123}I-MIBG uptake in patients with PD is significantly lower than that in patients with other parkinsonian syndromes [1–7]; this result corresponds to our results. Several reports suggest that the severity of motor impairment and disease duration are correlated with reduced ^{123}I-MIBG uptake in patients with PD [1, 2, 5, 6]; however, some other findings deny such correlations, similar to ours [3, 4, 7, 8]. This discrepancy is presumably explained by the fact that the degree of cardiac ^{123}I-MIBG uptake in patients in HY 1 and 2 of PD varies greatly among different studies. Difficult definitive diagnosis of PD in early and mild cases may also be because of the great variation. On the other hand, almost all patients in the advanced stage of PD have shown very low ^{123}I-MIBG uptake in both the previous and the present studies. Li et al. reported that cardiac sympathetic denervation progresses over time and that the rate of decrease in the number of sympathetic terminals appears to be at least as high as that of nigrostriatal dopaminergic terminals [35]. Therefore, we considered that although the onset of cardiac sympathetic denervation varied among the patients with PD, severe cardiac sympathetic denervation occurred in all of the patients by the terminal stage of PD. In regard to the association with a sympathetic symptom, it was reported that reduced ^{123}I-MIBG uptake does not always mean the existence of a sympathetic symptom [1, 3, 4, 7]. Also in this study, of the three patients in stage 4 of the HY scale who showed very low ^{123}I-MIBG uptake (Fig. 3), two had orthostatic hypotension; however, the remaining one patient had no cardiovascular sympathetic symptom and showed no abnormality in the head-up tilt test. In contrast to ^{123}I-MIBG uptake, the decrease in ^{11}C-CFT uptake in the whole striatum and in each of its three subregions significantly correlated with disease progression represented by the HY stages, as reported previously [14, 16, 22]. Considering the causal pathophysiological mechanism of PD, this is reasonable because ^{11}C-CFT uptake directly indicates nigrostriatal dopaminergic function.

We investigated the sensitivity and specificity of cardiac ^{123}I-MIBG scintigraphy in diagnosing PD and differentiating the patients with PD from the other patients with chief complaints of parkinsonian symptoms. Similar to the

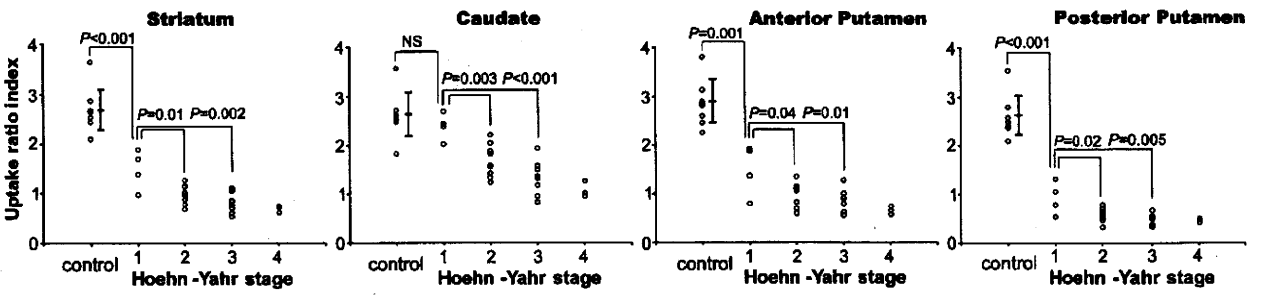

Fig. 4 Relation between the HY stage and uptake ratio index of ^{11}C-CFT in the whole striatum, caudate, anterior putamen and posterior putamen of patients with PD. In all four graphs, the uptakes in the patients in HY 1 of PD are significantly higher than those in the patients in HY 2 and 3 of PD. The uptakes in the caudate of patients in HY 1 of PD are not significantly higher than those in the caudate of controls, while the uptakes in the whole striatum, anterior putamen and posterior putamen of patients in HY 1 of PD are significantly higher than those in the corresponding regions of the controls. The *vertical bar* represents the mean ± SD of controls. *NS* not significant

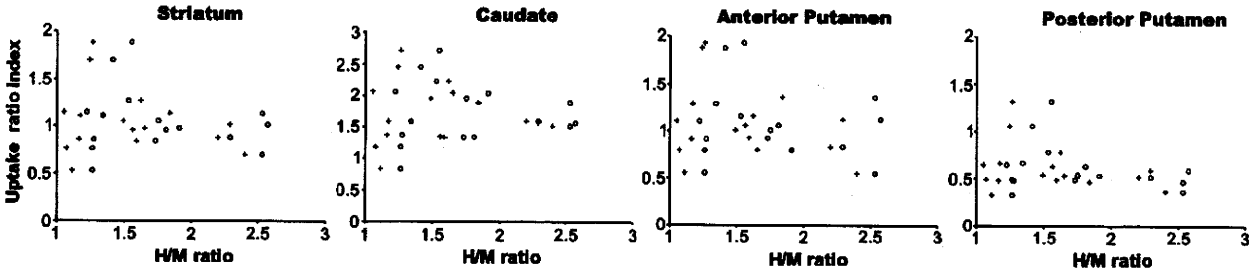

Fig. 5 Relation between the H/M ratio and uptake ratio index of ^{11}C-CFT in the whole striatum, caudate, anterior putamen and posterior putamen of patients with PD. Correlation was evaluated for 16 patients who underwent the two examinations (scintigraphy and PET) within 6 months. In all four graphs, no significant correlations are observed between the early images (*open circles*) and delayed images (*plus signs*)

previous meta-analysis of studies with a total of 246 PD cases [36], in both early and delayed images our study showed high specificity for the overall cases and high sensitivity for the advanced cases. However, early cases tended to have relatively lower sensitivity in both images, although the sample size and methodology greatly differed among the studies. Thus, our results suggested that even in the case of sustained cardiac ^{123}I-MIBG uptake, the possibility of PD should not be denied and follow-up clinical examinations, including ^{123}I-MIBG scintigraphy, should be conducted, especially in early and mild PD cases.

No definite correlation was found either between cardiac ^{123}I-MIBG uptake and striatal ^{11}C-CFT uptake or between cardiac ^{123}I-MIBG uptake and subregional ^{11}C-CFT uptake in the PD group. Two groups have reported the association between the functional impairment of the nigrostriatal dopaminergic system and that of the cardiac sympathetic system [8, 37]. Spiegel et al. (n=18) found a correlation between the two indices, i.e. ^{123}I-MIBG and ^{11}C-CFT uptake, while Raffel et al. (n=9) found no correlation between them. This discrepancy may be explained as follows. The functional impairment of both the nigrostriatal dopaminergic and cardiac sympathetic systems increases with disease progression, as described earlier; hence, a correlation was observed in some studies. On the other hand, there is no report that suggests a direct cause-effect relationship between the functional impairment of the nigrostriatal dopaminergic system and that of the cardiac sympathetic system. Thus, a statistically significant correlation between the functional impairments of the two systems may depend on the sample size and methodology. However, the functional impairments of the two systems would, in fact, occur and progress independently. Sometimes, impairment of the cardiac sympathetic function may precede that of the nigrostriatal dopaminergic function, while at other times, the latter may precede the former.

This is the first report wherein PD and NPD patterns in dopamine PET findings were defined on the basis of the results which have been confirmed as follows. In presynaptic DAT images, three characteristic changes are observed [14–16, 22]. First, the reduction in the ^{11}C-CFT uptake in the striatum begins from the posterior putamen, representing the initial locus of PD [38]. Second, the uptake ratio of the posterior putamen to the caudate is less than 1. Third, one putamen is usually more affected than the other, reflecting asymmetric degeneration. In fact, Fig. 4 shows that the ^{11}C-CFT uptake in the posterior putamen markedly decreased in the early stage of PD, while that in the caudate was relatively constant in the early stage. In postsynaptic D_2R images, putaminal uptake is normal or mildly upregulated in untreated PD, presumably as a compensatory response to decrease in presynaptic dopamine [17–19]. On the other hand, in treated or longstanding PD, the uptake restores to the normal level in the putamen and most often decreases in the caudate; this is presumably as a result of long-term downregulation due to chronic dopaminergic therapy or structural adaptation of the postsynaptic dopaminergic system to the progressive degeneration of nigrostriatal neurons [17, 19, 21]. In fact, in vitro studies have reported that the densities of striatal D_2Rs are maintained even in the advanced stage [39, 40].

On the basis of the earlier mentioned characteristic changes, especially in the posterior putamen, we defined the PD and NPD patterns such that false-negative cases should be as few as possible, because the aim was to reinforce the published clinical criteria. For defining the PD pattern, we considered that ^{11}C-CFT uptake in the posterior putamen of the patients should be less than that in the caudate of the patients and less than 50% of the mean uptake in normal controls. This percentage (i.e. 50%) was selected (1) on the basis of previous PET reports and considered suitable to distinguish normal from affected individuals [14–16, 22] and (2) on the basis of previous reports of in vitro studies, stating that parkinsonian symptoms appear when 80% of the striatal dopamine is lost or 50% of the nigral cells degenerate [38, 41]. Asymmetric uptake was not defined because of the difficulty in determining the intraindividual differences in

the uptake on the left and right sides. However, all 24 patients with PD showed asymmetric uptake. In the ^{11}C-raclopride PET image, since the uptake in the putamen was not less than the normal range, we considered that the uptake in the posterior putamen was normal or increased. For defining the NPD pattern, presynaptic function was not determined because the degree of the presynaptic dysfunction varies with diseases. In the ^{11}C-raclopride PET image, we considered that the uptake in the posterior putamen was normal or decreased because the uptake was not more than the normal range, except for Lewy body disease.

Conclusions

In early and mild PD cases, cardiac ^{123}I-MIBG scintigraphy is of limited value in the diagnosis of PD, because the sensitivity was indicated to be less than 70%. However, because of its high specificity for the overall cases and high sensitivity for the advanced cases, cardiac ^{123}I-MIBG scintigraphy may assist in the diagnosis of PD in a complementary role with the dopaminergic neuroimaging. Disease progression indicated by the HY stages has a stronger association with the nigrostriatal dopaminergic function assessed by striatal ^{11}C-CFT uptake than with the cardiac sympathetic function assessed by cardiac ^{123}I-MIBG uptake. The impairment of the two functions would occur and progress independently.

Acknowledgments The authors thank Mr. Keiichi Kawasaki, Dr. Masaya Hashimoto, and Ms. Hiroko Tsukinari for their technical assistance and useful discussions. This work was supported by grant-in-aid for Scientific Research (B) No. 20390334 (Ki.I.) from the Japan Society for the Promotion of Science and a grant (06-46) (Ki.I.) from the Program for Promotion of Fundamental Studies in Health Sciences of the National Institute of Biomedical Innovation of Japan, and a grant-in-aid for Neurological and Psychiatric Research (S.M., Y.S., and Ke.I.), and Research fo Longevity (S.M., Y.S., and Ke.I.) from the Ministry of Health, Labor, and Welfare of Japan, a grant-in-aid for Long-Term Comprehensive Research on Age-associated Dementia from the Tokyo Metropolitan Institute of Gerontology (K.K., S.M., and Ke.I.).

References

1. Orimo S, Ozawa E, Nakade S, Sugimoto T, Mizusawa H. (123)I-metaiodobenzylguanidine myocardial scintigraphy in Parkinson's disease. J Neurol Neurosurg Psychiatry 1999;67:189–94.
2. Satoh A, Serita T, Seto M, Tomita I, Satoh H, Iwanaga K, et al. Loss of 123I-MIBG uptake by the heart in Parkinson's disease: assessment of cardiac sympathetic denervation and diagnostic value. J Nucl Med 1999;40:371–5.
3. Taki J, Nakajima K, Hwang EH, Matsunari I, Komai K, Yoshita M, et al. Peripheral sympathetic dysfunction in patients with Parkinson's disease without autonomic failure is heart selective and disease specific. taki@med.kanazawa-u.ac.jp. Eur J Nucl Med 2000;27:566–73.
4. Takatsu H, Nishida H, Matsuo H, Watanabe S, Nagashima K, Wada H, et al. Cardiac sympathetic denervation from the early stage of Parkinson's disease: clinical and experimental studies with radiolabeled MIBG. J Nucl Med 2000;41:71–7.
5. Nagayama H, Hamamoto M, Ueda M, Nagashima J, Katayama Y. Reliability of MIBG myocardial scintigraphy in the diagnosis of Parkinson's disease. J Neurol Neurosurg Psychiatry 2005;76:249–51.
6. Hamada K, Hirayama M, Watanabe H, Kobayashi R, Ito H, Ieda T, et al. Onset age and severity of motor impairment are associated with reduction of myocardial 123I-MIBG uptake in Parkinson's disease. J Neurol Neurosurg Psychiatry 2003;74:423–6.
7. Braune S, Reinhardt M, Schnitzer R, Riedel A, Lucking CH. Cardiac uptake of [123I]MIBG separates Parkinson's disease from multiple system atrophy. Neurology 1999;53:1020–5.
8. Raffel DM, Koeppe RA, Little R, Wang CN, Liu S, Junck L, et al. PET measurement of cardiac and nigrostriatal denervation in Parkinsonian syndromes. J Nucl Med 2006;47:1769–77.
9. Rajput AH, Rozdilsky B, Rajput A. Accuracy of clinical diagnosis in parkinsonism–a prospective study. Can J Neurol Sci 1991;18:275–8.
10. Hughes AJ, Daniel SE, Kilford L, Lees AJ. Accuracy of clinical diagnosis of idiopathic Parkinson's disease: a clinico-pathological study of 100 cases. J Neurol Neurosurg Psychiatry 1992;55:181–4.
11. Jankovic J, Rajput AH, McDermott MP, Perl DP. The evolution of diagnosis in early Parkinson disease. Parkinson Study Group. Arch Neurol 2000;57:369–72.
12. Hughes AJ, Daniel SE, Lees AJ. Improved accuracy of clinical diagnosis of Lewy body Parkinson's disease. Neurology 2001;57:1497–9.
13. Plotkin M, Amthauer H, Klaffke S, Kuhn A, Ludemann L, Arnold G, et al. Combined 123I-FP-CIT and 123I-IBZM SPECT for the diagnosis of parkinsonian syndromes: study on 72 patients. J Neural Transm 2005;112:677–92.
14. Nurmi E, Bergman J, Eskola O, Solin O, Vahlberg T, Sonninen P, et al. Progression of dopaminergic hypofunction in striatal subregions in Parkinson's disease using [18F]CFT PET. Synapse 2003;48:109–15.
15. Frost JJ, Rosier AJ, Reich SG, Smith JS, Ehlers MD, Snyder SH, et al. Positron emission tomographic imaging of the dopamine transporter with 11C-WIN 35,428 reveals marked declines in mild Parkinson's disease. Ann Neurol 1993;34:423–31.
16. Rinne JO, Ruottinen H, Bergman J, Haaparanta M, Sonninen P, Solin O. Usefulness of a dopamine transporter PET ligand [(18)F] beta-CFT in assessing disability in Parkinson's disease. J Neurol Neurosurg Psychiatry 1999;67:737–41.
17. Antonini A, Schwarz J, Oertel WH, Beer HF, Madeja UD, Leenders KL. [11C]raclopride and positron emission tomography in previously untreated patients with Parkinson's disease: influence of L-dopa and lisuride therapy on striatal dopamine D2-receptors. Neurology 1994;44:1325–9.
18. Kaasinen V, Ruottinen HM, Någren K, Lehikoinen P, Oikonen V, Rinne JO. Upregulation of putaminal dopamine D2 receptors in early Parkinson's disease: a comparative PET study with [11C] raclopride and [11C]N-methylspiperone. J Nucl Med 2000;41:65–70.
19. Rinne JO, Laihinen A, Rinne UK, Någren K, Bergman J, Ruotsalainen U. PET study on striatal dopamine D2 receptor changes during the progression of early Parkinson's disease. Mov Disord 1993;8:134–8.
20. Dentresangle C, Veyre L, Le Bars D, Pierre C, Lavenne F, Pollak P, et al. Striatal D2 dopamine receptor status in Parkinson's disease: an [18F]dopa and [11C]raclopride PET study. Mov Disord 1999;14:1025–30.
21. Antonini A, Schwarz J, Oertel WH, Pogarell O, Leenders KL. Long-term changes of striatal dopamine D2 receptors in patients

with Parkinson's disease: a study with positron emission tomography and [11C]raclopride. Mov Disord 1997;12:33–8.
22. Wang J, Zuo CT, Jiang YP, Guan YH, Chen ZP, Xiang JD, et al. 18F-FP-CIT PET imaging and SPM analysis of dopamine transporters in Parkinson's disease in various Hoehn & Yahr stages. J Neurol 2007;254:185–90.
23. Knudsen GM, Karlsborg M, Thomsen G, Krabbe K, Regeur L, Nygaard T, et al. Imaging of dopamine transporters and D2 receptors in patients with Parkinson's disease and multiple system atrophy. Eur J Nucl Med Mol Imaging 2004;31:1631–8.
24. Kim YJ, Ichise M, Ballinger JR, Vines D, Erami SS, Tatschida T, et al. Combination of dopamine transporter and D2 receptor SPECT in the diagnostic evaluation of PD, MSA, and PSP. Mov Disord 2002;17:303–12.
25. Verstappen CC, Bloem BR, Haaxma CA, Oyen WJ, Horstink MW. Diagnostic value of asymmetric striatal D2 receptor upregulation in Parkinson's disease: an [123I]IBZM and [123I]FP-CIT SPECT study. Eur J Nucl Med Mol Imaging 2007;34:502–7.
26. Fujiwara T, Watanuki S, Yamamoto S, Miyake M, Seo S, Itoh M, et al. Performance evaluation of a large axial field-of-view PET scanner: SET-2400W. Ann Nucl Med 1997;11:307–13.
27. Hashimoto M, Kawasaki K, Suzuki M, Mitani K, Murayama S, Mishina M, et al. Presynaptic and postsynaptic nigrostriatal dopaminergic functions in multiple system atrophy. Neuroreport 2008;19:145–50.
28. Ishibashi K, Ishii K, Oda K, Kawasaki K, Mizusawa H, Ishiwata K. Regional analysis of age-related decline in dopamine transporters and dopamine D2-like receptors in human striatum. Synapse 2009;63:282–90.
29. NK LO, Dolle F, Lundkvist C, Sandell J, Swahn CG, Vaufrey F, et al. Precursor synthesis and radiolabelling of the dopamine D2 receptor ligand [11C]raclopride from [11C]methyl triflate. J Labelled Compd Radiopharm 1999;42:1183–93.
30. Kawamura K, Oda K, Ishiwata K. Age-related changes of the [11C]CFT binding to the striatal dopamine transporters in the Fischer 344 rats: a PET study. Ann Nucl Med 2003;17:249–53.
31. Antonini A, Leenders KL, Reist H, Thomann R, Beer HF, Locher J. Effect of age on D2 dopamine receptors in normal human brain measured by positron emission tomography and 11C-raclopride. Arch Neurol 1993;50:474–80.
32. Nakajima K, Taki J, Tonami N, Hisada K. Decreased 123I-MIBG uptake and increased clearance in various cardiac diseases. Nucl Med Commun 1994;15:317–23.
33. Gilman S, Low PA, Quinn N, Albanese A, Ben-Shlomo Y, Fowler CJ, et al. Consensus statement on the diagnosis of multiple system atrophy. J Auton Nerv Syst 1998;74:189–92.
34. Litvan I, Agid Y, Calne D, Campbell G, Dubois B, Duvoisin RC, et al. Clinical research criteria for the diagnosis of progressive supranuclear palsy (Steele-Richardson-Olszewski syndrome): report of the NINDS-SPSP international workshop. Neurology 1996;47:1–9.
35. Li ST, Dendi R, Holmes C, Goldstein DS. Progressive loss of cardiac sympathetic innervation in Parkinson's disease. Ann Neurol 2002;52:220–3.
36. Braune S. The role of cardiac metaiodobenzylguanidine uptake in the differential diagnosis of parkinsonian syndromes. Clin Auton Res 2001;11:351–5.
37. Spiegel J, Mollers MO, Jost WH, Fuss G, Samnick S, Dillmann U, et al. FP-CIT and MIBG scintigraphy in early Parkinson's disease. Mov Disord 2005;20:552–61.
38. Fearnley JM, Lees AJ. Ageing and Parkinson's disease: substantia nigra regional selectivity. Brain 1991;114(Pt 5):2283–301.
39. Guttman M, Seeman P, Reynolds GP, Riederer P, Jellinger K, Tourtellotte WW. Dopamine D2 receptor density remains constant in treated Parkinson's disease. Ann Neurol 1986;19:487–92.
40. Bokobza B, Ruberg M, Scatton B, Javoy-Agid F, Agid Y. [3H] spiperone binding, dopamine and HVA concentrations in Parkinson's disease and supranuclear palsy. Eur J Pharmacol 1984;99:167–75.
41. Kish SJ, Shannak K, Hornykiewicz O. Uneven pattern of dopamine loss in the striatum of patients with idiopathic Parkinson's disease. Pathophysiologic and clinical implications. N Engl J Med 1988;318:876–80.

Acta Neurol Scand DOI: 10.1111/j.1600-0404.2009.01255.x

Copyright © 2009 The Authors
Journal compilation © 2009 Blackwell Munksgaard

ACTA NEUROLOGICA
SCANDINAVICA

Cerebrospinal fluid metabolite and nigrostriatal dopaminergic function in Parkinson's disease

Ishibashi K, Kanemaru K, Saito Y, Murayama S, Oda K, Ishiwata K, Mizusawa H, Ishii K. Cerebrospinal fluid metabolite and nigrostriatal dopaminergic function in Parkinson's disease.
Acta Neurol Scand: DOI: 10.1111/j.1600-0404.2009.01255.x.
© 2009 The Authors Journal compilation © 2009 Blackwell Munksgaard.

Objectives – To evaluate the association between cerebrospinal fluid (CSF) homovanillic acid (HVA) concentrations and nigrostriatal dopaminergic function assessed by positron emission tomography (PET) imaging with carbon-11-labeled 2β-carbomethoxy-3β-(4-fluorophenyl)-tropane (^{11}C-CFT), which can measure the dopamine transporter (DAT) density, in Parkinson's disease (PD). *Methods* – ^{11}C-CFT PET scans and CSF examinations were performed on 21 patients with PD, and six patients with non-parkinsonian syndromes (NPS) as a control group. *Results* – In the PD group, CSF HVA concentrations were significantly correlated with the striatal uptake of ^{11}C-CFT ($r = 0.76$, $P < 0.01$). However, in the NPS group, two indices were within the normal range. *Conclusions* – In PD, CSF HVA concentrations correlate with nigrostriatal dopaminergic function. Therefore, CSF HVA concentrations may be an additional surrogate marker for estimating the remaining nigrostriatal dopaminergic function in case that DAT imaging is unavailable.

K. Ishibashi[1,2], K. Kanemaru[3], Y. Saito[4], S. Murayama[5], K. Oda[2], K. Ishiwata[2], H. Mizusawa[1], K. Ishii[2]

[1]Department of Neurology and Neurological Science, Graduate School, Tokyo Medical and Dental University, Tokyo, Japan; [2]Positron Medical Center, Tokyo Metropolitan Institute of Gerontology, Tokyo, Japan; [3]Department of Neurology, Tokyo Metropolitan Geriatric Hospital, Tokyo, Japan; [4]Department of Pathology, Tokyo Metropolitan Geriatric Hospital, Tokyo, Japan; [5]Department of Neuropathology, Tokyo Metropolitan Institute of Gerontology, Tokyo, Japan

Key words: cerebrospinal fluid; dopamine transporter; homovanillic acid; Parkinson's disease; positron emission tomography; ^{11}C-CFT

Kenji Ishii, MD, Positron Medical Center, Tokyo Metropolitan Institute of Gerontology, 1-1 Nakacho, Itabashi-ku, Tokyo 173-0022, Japan
Tel.: +81 3 3964 3241
Fax: +81 3 3964 2188
e-mail: ishii@pet.tmig.or.jp

Accepted for publication June 25, 2009

Introduction

In humans, homovanillic acid (HVA) is the major end-product of dopamine metabolism. The HVA in the cerebrospinal fluid (CSF) is largely derived from the nigrostriatal dopaminergic pathway; therefore, HVA concentration in the CSF has been used as an index of dopamine synthesis and presumed to reflect nigrostriatal dopaminergic function. However, even with the availability of a rigorous collection protocol, especially with respect to puncture time and pre-procedural resting, considerable inter-individual and intra-individual variability has been reported with regard to the concentration of CSF HVA in subjects with normal nigrostriatal function (1–3). Therefore, the extent to which CSF HVA concentrations reflect the nigrostriatal dopaminergic function is still unknown, and no study has specifically elucidated the association between the concentration of CSF HVA and the function of nigrostriatal dopamine.

Many studies have shown that the concentration of CSF HVA substantially reduces in patients with Parkinson's disease (PD), which is a neurodegenerative disorder caused by nigrostriatal dopaminergic dysfunction (4–12). However, the extent of reduction also varied a great deal among patients with PD. Because of the variability, the relationship of clinical disability with CSF HVA concentrations and the accuracy of CSF HVA concentrations in differentiating PD from other parkinsonian syndromes have yet to be determined. Several authors have reported an inverse relationship between CSF HVA concentrations and the clinical severity (5–7, 10, 11), while others have denied such a relationship (9, 12, 13). Other neurodegenerative disorders caused by the dysfunction of nigrostriatal dopaminergic system, such as multiple system atrophy (MSA), progressive

supranuclear palsy (PSP) and corticobasal degeneration, also show the reductions of CSF HVA concentrations as compared to normal subjects (8, 14, 15). Therefore, the usefulness of measuring CSF HVA concentrations in daily clinical practice has not yet been established.

In order to address the physiological and pathophysiological backgrounds of these issues, we evaluated the correlation between CSF HVA concentrations and nigrostriatal dopaminergic function. Furthermore, we have discussed the mechanism by which the concentration of CSF HVA reduces in patients with PD.

As means of evaluating nigrostriatal dopaminergic function, we performed carbon-11-labeled 2β-carbomethoxy-3β-(4-fluorophenyl)-tropane (^{11}C-CFT) positron emission tomography (PET) scans which can reveal the dopamine transporter (DAT) density in the striatum. DAT imaging has been recognized as a standard marker for the diagnosis of PD, because it is a very sensitive, reproducible, and reliable marker of nigrostriatal dopaminergic function (16–21).

Materials and methods

Subjects

The present study was a retrospective study. The subjects comprised 35 patients [19 men and 16 women; age 60–83 years (mean age = 71.7 years, SD = 6.0)]. They visited the neurological outpatient clinic at Tokyo Metropolitan Geriatric Hospital from April 2001–November 2004. Of the 35 patients, 29 had parkinsonian symptoms and on the basis of each clinical criteria (22–24), 21 were diagnosed with PD, three with MSA, and five with PSP. The remaining six patients had no parkinsonian symptoms: three were clinically diagnosed with Alzheimer's disease (AD), two with spinocerebellar degeneration (SCD), and one with amyotrophic lateral sclerosis (ALS). Table 1 shows the demographic data. The patients with MSA and PSP were classified in the patients with non-PD (NPD) group, while the patients with AD, SCD and ALS were classified in the patients with non-parkinsonian syndromes (NPS) group. The CSF examinations and the ^{11}C-CFT PET scans were performed within 5 months of each other. None of the patients had any concomitant hereditary disorder that could cause parkinsonian symptoms. All the patients were drug naive.

The normal range of HVA was determined by examining the CSF of 13 normal control subjects [five men and eight women; age, 65–88 years (mean = 77.2 years, SD = 8.2)]. Similarly, the normal range for nigrostriatal dopaminergic function was determined by performing ^{11}C-CFT PET scans of eight normal control subjects [five men and three women; age, 55–74 years (mean age = 62.3 years, SD = 6.9)]. All the control subjects were healthy and did not have any underlying diseases or abnormities, as determined on the basis of their medical history and their physical and neurological examinations. None of them were on any medications at the time of the study. All the subjects also underwent routine MRI examinations.

All the CSF examinations and ^{11}C-CFT PET scans were performed for research. This study protocol was approved by the Ethics Committee of the Tokyo Metropolitan Institute of Gerontology and written informed consents were obtained from all the participants.

CSF analysis

Lumbar puncture was performed in the lateral decubitus position to obtain CSF samples from each subject. The first few milliliter of CFS was discarded. The next 3 ml of CFS was used for routine determinations of cell counts, protein and sugar and an additional 2 ml was stored at −70°C until the assays were preformed. The concentration of CSF HVA was measured by injecting 80 μl CSF

Table 1 Demographics of patients and control subjects

	Subjects				Striatal uptake of ^{11}C-CFT	
	n	M:F	Age (years)	Duration (years)	(Uptake ratio index)	CSF HVA (ng/ml)
Parkinson's disease	21	11:10	72.9 ± 5.0	1.8 ± 1.3	0.94 ± 0.20	12.8 ± 9.35
Hoehn-Yahr 1	1	1:0	62	1	1.38	36.8
Hoehn-Yahr 2	8	4:4	71.6 ± 4.6	1.4 ± 0.9	1.03 ± 0.14	15.6 ± 9.4
Hoehn-Yahr 3	12	6:6	74.7 ± 3.9	2.1 ± 1.5	0.85 ± 0.17	8.9 ± 5.4
Non-Parkinson's disease	8	4:4	70.5 ± 7.7	1.6 ± 0.8	1.00 ± 0.19	16.4 ± 7.7
Non-parkinsonian syndromes	6	4:2	68.8 ± 6.3	4.5 ± 2.4	2.48 ± 0.28	31.9 ± 13.0
Control for PET study	8	5:3	62.3 ± 6.9		2.68 ± 0.44	
Control for CSF study	13	5:8	77.2 ± 8.2			36.0 ± 13.8

Data are expressed as mean ± SD; *n* = number, CSF, cerebrospinal fluid; HVA, homovanillic acid.

samples into a high-performance liquid chromatography system equipped with 16 electrochemical sensors (CEAS Model 5500; ESA, Bedford, MA, USA), as described previously (14).

PET imaging

^{11}C-CFT PET data acquisition – PET studies were performed at the Positron Medical Center, Tokyo Metropolitan Institute of Gerontology using a SET 2400W scanner (Shimadzu, Kyoto, Japan) in the three-dimensional scanning mode (25). The ^{11}C-CFT was prepared as described previously (26). Each subject received an intravenous bolus injection of 388 ± 75 (mean ± SD) MBq of ^{11}C-CFT. Each subject was then placed in the supine position with their eyes closed in the PET camera gantry. The head was immobilized with a customized head holder in order to align the orbitomeatal line parallel to the scanning plane. To measure the uptake of ^{11}C-CFT, a static scan was performed for 75–90 min after the injection. The specific activity at the time of injection ranged from 7.1–119.6 GBq/μmol. The transmission data were acquired using a rotating ^{68}Ga/^{68}Ge rod source for attenuation correction. Images of 50 slices were obtained with a resolution of 2 × 2 × 3.125 mm voxels and a 128 × 128 matrix.

Analysis of ^{11}C-CFT PET images – Image manipulations were carried out by using the Dr View software (version R2.0; AJS, Tokyo, Japan). The individual PET images were resliced in the transaxial direction, parallel to the anterior–posterior intercommissural (AC–PC) line. Circular regions of interest (ROIs) were placed with reference to the brain atlas and individual MRI images. Five ROIs (diameter, 8 mm) were placed on the striatum on both the left and right sides in each of the three contiguous slices (the AC–PC plane, and regions 3.1 and 6.2 mm above the AC–PC line). Of the five ROIs, one ROI was placed on the caudate and four on the putamen. A total of 50 ROIs (diameter, 10 mm) were selected throughout the cerebellar cortex in five contiguous slices. To evaluate the striatal uptake of ^{11}C-CFT, we calculated the uptake ratio index by the following formula (17, 18), as previously validated (27, 28).

$$\text{Uptake ratio index} = (\text{activity in the striatum} - \text{activity in the cerebellum}) / (\text{activity in the cerebellum}).$$

Statistical analysis

Differences in the averages were tested using a Student's *t*-test. Correlations between the two groups were assessed by linear regression analysis with Pearson's correlation test. $P < 0.01$ was considered to indicate statistical significance.

Results

The inter-individual variability in the concentrations of CSF HVA in each group was relatively large (Fig. 1A). CSF HVA concentrations in both the PD ($P < 0.01$) and NPD groups ($P < 0.01$) were significantly lower than that in the control group (mean ± 2SD, 36.0 ± 27.6), while no significant difference was observed between the NPS and control groups.

The striatal uptake of ^{11}C-CFT in the PD and NPD groups was below the normal range (mean ± 2SD, 2.68 ± 0.87; Fig. 1B). In the PD group, CSF HVA concentrations were significantly

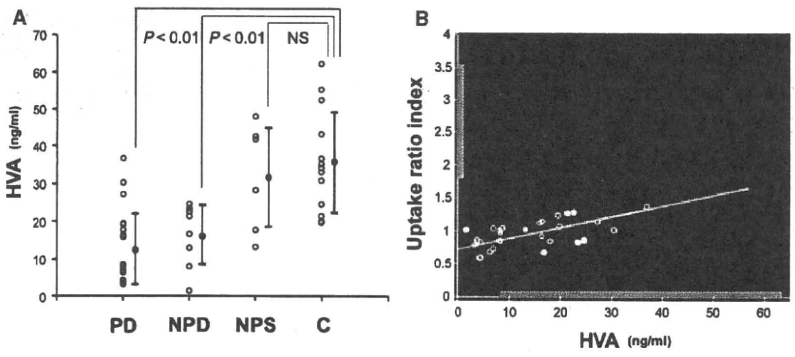

Figure 1. (A) The comparison of CSF HVA concentrations among the disease and control groups. Vertical bars represent mean ± SD. (B) Relationship between CSF HVA concentrations and the striatal uptake of ^{11}C-CFT. A solid line represents the regression line for the PD group. Linear correlation was significant ($r = 0.76$; $P < 0.01$). The grey bars beside the *x*- and *y*-axes represent the normal range (mean ± 2SD) for HVA (36.0 ± 27.6) and the striatal uptake of ^{11}C-CFT (2.68 ± 0.87). PD, Parkinson's disease; NPD, non-Parkinson's disease with parkinsonism; NPS, non-parkinsonian syndromes; C, controls; NS, not significant; CSF, cerebrospinal fluid; HVA, homovanillic acid.

correlated with the striatal uptake of ^{11}C-CFT ($r = 0.76$, $P < 0.01$). In the NPD group, although the correlation between the two indices was not statistically significant, the distribution pattern between the two indexes showed the same tendency as that in the PD group. However, in the NPS group, both CSF HVA concentrations and the striatal uptake of ^{11}C-CFT were within the normal ranges.

Discussion

We evaluated the correlation between CSF HVA concentrations and nigrostriatal dopaminergic function by performing ^{11}C-CFT PET scans. ^{11}C-CFT PET scans showed that all patients with PD and NPD had the dysfunction of nigrostriatal dopaminergic system and all patients with NPS had normal function. The CSF HVA concentrations of all patients with PD and NPD were significantly lower than those of normal subjects, in accordance with previous studies (5–12, 14, 15), whereas, there was no significant difference in CSF HVA concentrations between normal subjects and patients with NPS. These results suggest that CSF HVA concentrations could reflect nigrostriatal dopaminergic function. However, in accordance with previous reports (1–9, 13, 14), all groups showed large inter-individual variability in CSF HVA concentrations and relatively wide overlaps among groups were found. Therefore, in clinical practice, measuring CSF HVA concentrations may be of limited value in the diagnosis of PD.

This is the first study that investigated the correlation between CSF HVA concentrations and nigrostriatal dopaminergic dysfunction. Regardless of relatively high inter-individual variability, CSF HVA concentrations in the PD group showed a considerably high correlation with the striatal uptake of ^{11}C-CFT. The NPD group with nigrostriatal dopaminergic dysfunction showed the same tendency as the PD group, although without significant correlation probably because of the small number of patients. On the other hand, the NPD group with normal nigrostriatal dopaminergic function showed normal ranges in both the HVA level and the striatal uptake of ^{11}C-CFT. Therefore, CSF HVA concentrations may be an additional surrogate maker for estimating the nigrostriatal dopaminergic function in patients with PD, in case that DAT imaging, which has been recognized as a standard maker for the diagnosis of PD, is unavailable.

It is important to note that the DAT images of patients with PD are unique; in the pre-symptomatic phase the reduction in the availability of striatal DAT was detected, presumably as a result of both the degeneration of nigral dopaminergic cells and the compensatory downregulation of DATs on the presynaptic site to maintain normal synaptic dopamine concentrations (17–21). Furthermore, the striatal DAT availability declined at an annual rate of 5–10% (19, 21, 29–31).

Considering our results and the unique characteristics of the DAT images, a possible explanation about the association between CSF HVA concentrations and the striatal uptake of ^{11}C-CFT is as follows (Fig. 2). The first stage of the disease is a compensatory and asymptomatic phase. Along with the progression of nigrostriatal degeneration, the striatal DAT availability begins to decrease, as described earlier (17–21). However, due to several compensatory mechanisms, including the downregulation of DATs and the upregulation of dopamine synthesis, the striatal dopamine concentrations are kept within the normal range (32). As a result, CSF HVA concentrations are also kept in the normal range because CSF HVA is the major end-product of striatal dopamine metabolism. This phase would show relatively large intra-individual and inter-individual variability in CSF HVA concentrations, as observed in subjects with normal nigrostriatal dopaminergic function, because of the reserve capacity for adjusting its levels. The second stage of the progression of the disease is an advanced and symptomatic phase. The compensatory mechanisms to maintain normal synaptic

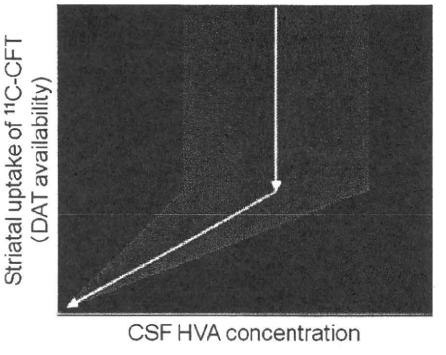

Figure 2. Schematic representation of the mechanism of CSF HVA reduction in patients with PD. (A) The nigrostriatal degeneration begins with a decrease in DAT availability, but due to several compensatory mechanisms, striatal dopamine concentrations (CSF HVA concentrations) are maintained within the normal range. There is a large variability with regard to CSF HVA concentrations. (B) The compensatory mechanisms break down and striatal dopamine concentrations (CSF HVA concentrations) begin to decrease along with the decrease in DAT availability. The variability in CSF HVA concentrations gradually becomes smaller. The grey zone represents the range of variability in CSF HVA concentrations to the striatal uptake of ^{11}C-CFT. DAT, dopamine transporter; CSF, cerebrospinal fluid, HVA, homovanillic acid.

dopamine concentrations break down and the striatal dopamine and CSF HVA concentrations begin to decrease with the reduction of DAT availability. In this phase, the intra-individual and inter-individual variability in CSF HVA concentrations would gradually decrease because of a lesser capacity for adjusting its levels. Consequently, CSF HVA concentrations remain within a narrow range that corresponds to the remaining nigrostriatal dopaminergic function. In symptomatic patients with PD, CSF HVA concentrations correlate with nigrostriatal dopaminergic function. To verify this explanation, a study with larger number of patients is needed.

In conclusion, we found a significant correlation between CSF HVA concentrations and the striatal uptake of ^{11}C-CFT in patients with PD. Although we should remember that CSF HVA concentrations show large variability, CSF HVA concentrations may be an additional surrogate maker for estimating the remaining nigrostriatal dopaminergic function in patients with PD in case that DAT imaging is unavailable.

Acknowledgements

The authors thank Mr Keiichi Kawasaki and Ms Hiroko Tsukinari for their technical assistance. This study was supported by Grants-in-Aid for Neurological and Psychiatric Research (S. Murayama, Y. Saito and K. Ishii) and Research for Longevity (S. Murayama, Y. Saito and K. Ishii) from the Ministry of Health, Labor and Welfare of Japan; for Scientific Research (B) No. 20390334 (K. Ishiwata) from the Japan Society for the Promotion of Science; for the Program for Promotion of Fundamental Studies in Health Sciences of the National Institute of Biomedical Innovation, Japan (No: 06–46, K. Ishiwata); and for Long-Term Comprehensive Research on Age-associated Dementia from the Tokyo Metropolitan Institute of Gerontology (K. Kanemaru, S. Murayama and K. Ishii).

References

1. Seeldrayers P, Messina D, Desmedt D, Dalesio O, Hildebrand J. CSF levels of neurotransmitters in Alzheimer-type dementia. Effects of ergoloid mesylate. Acta Neurol Scand 1985;**71**:411–4.
2. Ballenger JC, Post RM, Goodwin FK. Neurochemistry of cerebrospinal fluid in normal individuals. In: Wood JH, ed. Neurobiology of cerebrospinal fluid. New York: Plenum Press, 1982;2:143–55.
3. Hildebrand J, Bourgeois F, Buyse M, Przedborski S, Goldman S. Reproducibility of monoamine metabolite measurements in human cerebrospinal fluid. Acta Neurol Scand 1990;**81**:427–30.
4. Parkinson Study Group. Cerebrospinal fluid homovanillic acid in the DATATOP study on Parkinson's disease. Parkinson Study Group. Arch Neurol 1995;**52**:237–45.
5. Chia LG, Cheng FC, Kuo JS. Monoamines and their metabolites in plasma and lumbar cerebrospinal fluid of Chinese patients with Parkinson's disease. J Neurol Sci 1993;**116**:125–34.
6. Chase TN, Ng LK. Central monoamine metabolism in Parkinson's disease. Arch Neurol 1972;**27**:486–91.
7. Korf J, van Praag HM, Schut D, Nienhuis RJ, Lakke JP. Parkinson's disease and amine metabolites in cerebrospinal fluid: implications for L-Dopa therapy. Eur Neurol 1974; **12**:340–50.
8. Abdo WF, De Jong D, Hendriks JC et al. Cerebrospinal fluid analysis differentiates multiple system atrophy from Parkinson's disease. Mov Disord 2003;**19**:571–9.
9. Davidson DL, Yates CM, Mawdsley C, Pullar IA, Wilson H. CSF studies on the relationship between dopamine and 5-hydroxytryptamine in Parkinsonism and other movement disorders. J Neurol Neurosurg Psychiatry 1977;**40**: 1136–41.
10. Tohgi H, Abe T, Takahashi S, Ueno M, Nozaki Y. Cerebrospinal fluid dopamine, norepinephrine, and epinephrine concentrations in Parkinson's disease correlated with clinical symptoms. Adv Neurol 1990;**53**:277–82.
11. Mayeux R, Stern Y. Intellectual dysfunction and dementia in Parkinson disease. Adv Neurol 1983;**38**:211–27.
12. Gibson CJ, Logue M, Growdon JH. CSF monoamine metabolite levels in Alzheimer's and Parkinson's disease. Arch Neurol 1985;**42**:489–92.
13. Kurlan R, Goldblatt D, Zaczek R et al. Cerebrospinal fluid homovanillic acid and parkinsonism in Huntington's disease. Ann Neurol 1988;**24**:282–4.
14. Kanemaru K, Mitani K, Yamanouchi H. Cerebrospinal fluid homovanillic acid levels are not reduced in early corticobasal degeneration. Neurosci Lett 1998;**245**:121–2.
15. Ruberg M, Javoy-Agid F, Hirsch E et al. Dopaminergic and cholinergic lesions in progressive supranuclear palsy. Ann Neurol 1985;**18**:523–9.
16. Nurmi E, Bergman J, Eskola O et al. Reproducibility and effect of levodopa on dopamine transporter function measurements: a [18F]CFT PET study. J Cereb Blood Flow Metab 2000;**20**:1604–9.
17. Frost JJ, Rosier AJ, Reich SG et al. Positron emission tomographic imaging of the dopamine transporter with 11C-WIN 35,428 reveals marked declines in mild Parkinson's disease. Ann Neurol 1993;**34**:423–31.
18. Wong DF, Yung B, Dannals RF et al. In vivo imaging of baboon and human dopamine transporters by positron emission tomography using [11C]WIN 35,428. Synapse 1993;**15**:130–42.
19. Nurmi E, Bergman J, Eskola O et al. Progression of dopaminergic hypofunction in striatal subregions in Parkinson's disease using [18F]CFT PET. Synapse 2003; **48**:109–15.
20. Rinne JO, Ruottinen H, Bergman J, Haaparanta M, Sonninen P, Solin O. Usefulness of a dopamine transporter PET ligand [(18)F]beta-CFT in assessing disability in Parkinson's disease. J Neurol Neurosurg Psychiatry 1999;**67**:737–41.
21. Nurmi E, Ruottinen HM, Kaasinen V et al. Progression in Parkinson's disease: a positron emission tomography study with a dopamine transporter ligand [18F]CFT. Ann Neurol 2000;**47**:804–8.
22. Hughes AJ, Daniel SE, Kilford L, Lees AJ. Accuracy of clinical diagnosis of idiopathic Parkinson's disease: a clinico-pathological study of 100 cases. J Neurol Neurosurg Psychiatry 1992;**55**:181–4.
23. Litvan I, Agid Y, Calne D et al. Clinical research criteria for the diagnosis of progressive supranuclear palsy (Steele-Richardson-Olszewski syndrome): report of the NINDS-SPSP international workshop. Neurology 1996; **47**:1–9.

24. Gilman S, Low PA, Quinn N et al. Consensus statement on the diagnosis of multiple system atrophy. J Auton Nerv Syst 1998;**74**:189–92.
25. Fujiwara T, Watanuki S, Yamamoto S et al. Performance evaluation of a large axial field-of-view PET scanner: SET-2400W. Ann Nucl Med 1997;**11**:307–13.
26. Kawamura K, Oda K, Ishiwata K. Age-related changes of the [11C]CFT binding to the striatal dopamine transporters in the Fischer 344 rats: a PET study. Ann Nucl Med 2003;**17**:249–53.
27. Hashimoto M, Kawasaki K, Suzuki M et al. Presynaptic and postsynaptic nigrostriatal dopaminergic functions in multiple system atrophy. Neuroreport 2008;**19**:145–50.
28. Ishibashi K, Ishii K, Oda K, Kawasaki K, Mizusawa H, Ishiwata K. Regional analysis of age-related decline in dopamine transporters and dopamine D(2)-like receptors in human striatum. Synapse 2008;**63**:282–90.
29. Staffen W, Mair A, Unterrainer J, Trinka E, Ladurner G. Measuring the progression of idiopathic Parkinson's disease with [123I] beta-CIT SPECT. J Neural Transm 2000; **107**:543–52.
30. Chouker M, Tatsch K, Linke R, Pogarell O, Hahn K, Schwarz J. Striatal dopamine transporter binding in early to moderately advanced Parkinson's disease: monitoring of disease progression over 2 years. Nucl Med Commun 2001;**22**:721–5.
31. Marek K, Innis R, van Dyck C et al. [123I]beta-CIT SPECT imaging assessment of the rate of Parkinson's disease progression. Neurology 2001;**57**:2089–94.
32. Lee CS, Samii A, Sossi V et al. In vivo positron emission tomographic evidence for compensatory changes in presynaptic dopaminergic nerve terminals in Parkinson's disease. Ann Neurol 2000;**47**:493–503.

Clinical/Scientific Notes

T. Shishido, MD
M. Ikemura, MD, PhD
T. Obi, MD, PhD
K. Yamazaki, MD, PhD
T. Terada, MD
A. Sugiura, MD
Y. Saito, MD, PhD
S. Murayama, MD, PhD
K. Mizoguchi, MD, PhD

α-SYNUCLEIN ACCUMULATION IN SKIN NERVE FIBERS REVEALED BY SKIN BIOPSY IN PURE AUTONOMIC FAILURE

Pure autonomic failure (PAF), a rare clinical manifestation of Lewy body (LB) disorders, is characterized by fibrillary aggregates of α-synuclein in the cytoplasm of a select population of neurons and glia. It is a sporadic, idiopathic, neurodegenerative disorder with orthostatic hypotension as the cardinal symptom. Patients may also present with decreased sweating, urinary dysfunction, constipation, and sexual dysfunction. Postmortem studies[1-3] have disclosed prominent LB pathology in sympathetic and parasympathetic nervous systems, as well as the substantia nigra and locus ceruleus. Here, we show for the first time α-synuclein accumulation in nerve fibers in the dermis of a patient with PAF.

The patient is a 73-year-old man with a 13-year history of severe orthostatic hypotension with recurrent syncope, urinary dysfunction (hesitancy and prolongation), erectile failure, and decreased sweating with heat intolerance. Supine blood pressure was 163/84 mm Hg. After 1 minute of a 60° head-up tilt test, the patient's blood pressure fell to 62/33 mm Hg and he fainted. The patient's pulse was 60 beats/minute before tilting and 65 beats/minute after 1 minute of tilting, and his plasma noradrenaline was 40 and 36 pg/mL before and after tilting, respectively (normal: >100 pg/mL). The coefficient of variation of R-R intervals was 0.81% (normal: >1.5%). Denervation supersensitivity to noradrenaline was detected with infusion testing. A thermoregulatory sweat test revealed a patchy lack of sweating in the legs. The heart-to-mediastinum (H/M) ratio of ^{131}I-metaiodobenzylguanidine (MIBG) myocardial scintigraphy was reduced (early: 1.30, late: 1.25, normal: >1.85).

After the patient provided informed consent, skin samples, 5 mm in diameter and including the dermis, were obtained from around his ankles, directly fixed in 10% buffered formalin for 24 hours, and cut into 6-μm-thick serial paraffin sections. The sections were stained with hematoxylin and eosin and also stained immunohistochemically with an autoimmunostainer (20NX, Ventana, Tucson, AZ) and antiphosphorylated α-synuclein (psyn) antibodies (psyn#64 monoclonal and PSer129 polyclonal, gifts from Dr T. Iwatsubo, University of Tokyo). We also stained alternating serial sections with polyclonal anti-psyn and antiphosphorylated neurofilament antibodies (SMI31 monoclonal, Sternberger Immunochemicals, Bethesda, MD) to show the axons. Additional sections were immunostained with anti–tyrosine hydroxylase (TH) antibodies (Calbichem-Novabiochem Corporation, Darmstadt, Germany).

Anti-psyn immunohistochemistry showed positive neurites and dots in unmyelinated nerve fascicles of the dermis and subcutaneous tissue (figure, A and B). Small psyn-positive dots or thin linear structures were also found around blood vessels and were coincident with SMI31-immunoreactive axons (figure, C and D). TH immunostaining showed no immunoreactivity in the patient's nerve fascicles and blood vessel walls (figure, E and G), although sections from control subjects were TH-positive (figure, F and H).

Our patient fulfilled the criteria of the consensus statement on the definition of PAF.[4] Autonomic function tests indicated both sympathetic and parasympathetic involvement.

Skin α-synuclein has been detected by immunoblotting in some patients with Parkinson disease (PD),[5] and we have reported psyn-positive unmyelinated nerve fascicles in the skin of patients with PD and dementia with Lewy bodies (DLB), including aggregates within TH-immunoreactive axons and nonreactive axons.[6] Therefore, we biopsied the skin areas that showed no sweating in the thermoregulatory sweat test, because cutaneous sudomotor nerves contain unmyelinated adrenergic and cholinergic sympathetic nerve fibers that innervate blood vessels and sweat glands. The cutaneous unmyelinated nerve fascicles were immunoreactive for α-synuclein, and some extended into the walls of blood vessels. With absent TH immunoreactivity in nerve fascicles and blood vessel walls, dysfunction of sympathetic nerve fibers

Editorial, page 536

Copyright © by AAN Enterprises, Inc. Unauthorized reproduction of this article is prohibited.

Figure Immunostaining for α-synuclein and tyrosine hydroxylase in the skin

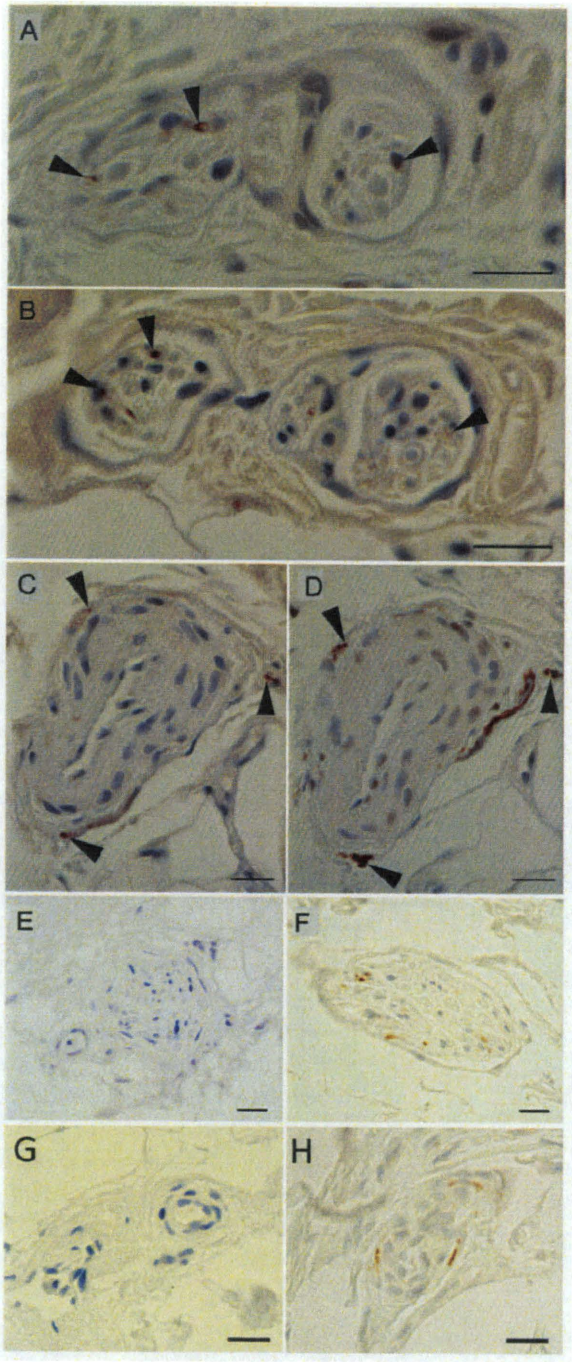

Immunohistochemical study of nerve fascicles and vascular walls in the skin around the patient's left ankle with antiphosphorylated α-synuclein (psyn) antibodies (A: psyn#64, monoclonal; B, C: PSer129, polyclonal), antiphosphorylated neurofilament antibodies (D: SMI31 monoclonal), and anti-tyrosine hydroxylase (TH) antibodies (E–H). A–H: bars = 20 μm. C and D are serial sections. (A, B) Dot-like psyn immunoreactivity (arrowheads) was present in a cross-section of a nerve fascicle. (C, D) Psyn immunoreactivity revealed dots and a thin linear structure (C, arrowheads), which was determined with SMI31 to be the wall of a blood vessel extending from a nerve fascicle (D, arrowheads). (E, F) TH immunoreactivity was absent in a cross-section of a nerve fascicle in this patient (E). In contrast, TH immunoreactivity was observed in a control subject (79-year-old man; F). (G, H) TH immunoreactivity was absent in a cross-section of a blood vessel wall in this patient (G). In contrast, TH immunoreactivity was detected in a control subject (89-year-old man; H). No erector pili muscle was observed in the skin of this patient.

may underlie this patient's hypohidrosis and could be caused by the α-synuclein aggregation.

In PD and DLB, α-synuclein aggregates in the distal axons of the cardiac sympathetic nerves provoke the degeneration of these nerves.[7] MIBG myocardial scintigraphy enables the quantification of postganglionic sympathetic cardiac innervation; the H/M ratio was reduced in our patient, suggesting that α-synuclein aggregation may also be the pathologic cause of cardiac sympathetic nervous system degeneration in PAF.

We have shown that LB-related pathology in the skin is always accompanied by LB-related pathology in the CNS and adrenal glands of patients with PD and DLB.[6] Thus, synuclein accumulation in cutaneous nerve fibers may indicate that this patient without parkinsonism also has LB–related pathology in the adrenal glands and brain. Indeed, varying amounts of LBs and neuronal loss occur in the substantia nigra, locus ceruleus, and adrenomedullary cells in patients with PAF.[1-3]

α-Synuclein pathology in cutaneous nerves in this patient provides additional evidence that PAF is an α-synucleinopathy. Examining biopsies of hypohidrotic skin for α-synuclein-positive cutaneous nerve fibers in a series of patients with PAF should be performed in the future.

From the Department of Neurology (T.S., T.O., K.Y., T.T., A.S., K.M.), Shizuoka Institute of Epilepsy and Neurological Disorders, Shizuoka; Department of Neuropathology (M.I., Y.S., S.M.), Tokyo Metropolitan Institute of Gerontology, Tokyo; and Department of Pathology (M.I.), Teikyo University School of Medicine, Tokyo, Japan.

Disclosure: Dr. Shishido, Dr. Ikemura, Dr. Obi, Dr. Yamazaki, Dr. Terada, Dr. Sugiura, and Dr. Saito report no disclosures. Dr. Murayama serves on the editorial board of Neuropathology *and receives research support from the Japanese Governmental Bureau of Health, Labor and Welfare. Dr. Mizoguchi reports no disclosures.*

Received April 28, 2009. Accepted in final form October 26, 2009.

Address correspondence and reprint requests to Dr. Tomokazu Obi, Department of Neurology, Shizuoka Institute of Epilepsy and Neurological Disorders, Urushiyama 886, Aoi-ku, Shizuoka 420-8688, Japan; obit@szec.hosp.go.jp

Copyright © 2010 by AAN Enterprises, Inc.

ACKNOWLEDGMENT

The authors thank Dr. Takeshi Iwatsubo (Department of Neuropathology, University of Tokyo) for the donation of antibodies.

1. Hague K, Lento P, Morgello S, Car S, Kaufmann H. The distribution of Lewy bodies in pure autonomic failure: autopsy findings and review of the literature. Acta Neuropathol 1997;94:192–196.
2. Arai K, Kato N, Kashiwado K, Hattori T. Pure autonomic failure in association with human α-synucleinopathy. Neurosci Lett 2000;296:171–173.
3. Kaufmann H, Hague K, Perl D. Accumulation of alpha-synuclein in autonomic nerves in pure autonomic failure. Neurology 2001;56:980–981.

4. Consensus Committee of the American Academy of Neurology. Consensus statement on the definition of orthostatic hypotension, pure autonomic fallure, and multiple system atrophy. Neurology 1996;46:1470.
5. Michell AW, Luheshi LM, Barker RA. Skin and platelet α-synuclein as peripheral biomarkers of Parkinson's disease. Neurosci Lett 2005;381:294–298.
6. Ikemura M, Saito Y, Sengoku R, et al. Lewy body pathology involves cutaneous nerves. J Neuropathol Exp Neurol 2008;67:945–953.
7. Mitsui J, Saito Y, Momose T, et al. Pathology of the sympathetic nervous system corresponding to the decreased cardiac uptake in 123I-metaiodobenzylguanidine (MIBG) scintigraphy in a patient with Parkinson disease. J Neurol Sci 2006;243:101–104.

Kate El Bouzidi, MB, ChB
Susan Duncan, MD, FRCP
Ian R. Whittle, PhD, FRCS
Christopher R. Butler, PhD, MRCP

LESIONAL REFLEX EPILEPSY ASSOCIATED WITH THE THOUGHT OF FOOD

A 44-year-old right-handed woman was walking in the Scottish highlands. Upon unwrapping her lunch, she had a focal seizure with witnessed onset on the right side of the face and secondary generalization. Postictally, she was aphasic with a right hemiparesis. She was airlifted to hospital. Sodium valproate was commenced, increasing to 700 mg twice daily, and she was discharged home. Three weeks later, the smell of food triggered another seizure and she was admitted to the neurology unit where carbamazepine was introduced (200 mg twice daily).

The next morning, the patient had a simple partial seizure after eating a spoonful of porridge and 3 more when eating lunch, a snack, and dinner. Thereafter, most meals triggered seizures, as did other food-related stimuli such as being offered a piece of cake, seeing her visitors pass around food at her bedside, and smelling the hospital dinner trolley. Fifty-four seizures occurred over the next 14 days and 50 were related to food. The episodes typically lasted 80 seconds and were characterized by a tingling sensation in the tongue and right-sided facial and tongue movements. Consciousness was unimpaired.

Thirty-four seizures occurred during the act of eating, always early on in the meal while the patient still felt hungry. Fifteen were precipitated by the sight or smell of food alone, 1 while browsing a recipe book, and 3 when she could smell her pet dog's food. One seizure was provoked by discussing cooking and another was triggered by the mint flavor of toothpaste. A single nocturnal seizure was accompanied by a strong feeling of nausea. The 2 other seizures associated with nonfood stimuli were related to stressful situations such as discussing a call from the doctor. Neither chewing movements nor speaking induced seizures.

Interictal EEG was normal. MRI revealed a nonenhancing lesion in the left premotor strip (figure).

The seizures were refractory to medical therapy. An awake frontoparietal craniotomy was performed with electrocorticography. Epileptiform activity was identified in the left frontal operculum, anterior and inferior to the lesion (figure). A subtotal resection was performed. Histopathology revealed a WHO grade IV glioblastoma. No reflex seizures occurred after surgery.

Discussion. We present a case of symptomatic reflex seizures triggered by food-related stimuli, with detailed neuroimaging and electrophysiologic localization of the epileptic focus. Reflex epilepsies are characterized by seizures consistently induced by a specific stimulus. Typically, they are idiopathic and generalized. Recognized stimuli include flashing lights, music, reading, toothbrushing, and eating. Over 200 cases of idiopathic eating epilepsy have been reported, many from South Asia, with a male preponderance and onset typically in the second decade of life.[1] In all cases, the act of eating was required to provoke seizures, which were focal or generalized. Of 128 cases in which treatment response is described, 48 (37.5%) became seizure-free, 64 (50%) achieved partial control of seizures, and 16 (12.5%) showed no benefit.[1,2]

There are far fewer reported cases of symptomatic eating epilepsy. The associated pathologies include congenital malformations, vascular abnormalities, postinfective lesions, and 1 neoplasm: an astrocytoma. Lesions involved the opercula, amygdalae, and temporoparietal lobes.[3,4] Most cases were refractory to medical therapy.

Rarer still are cases of reflex epilepsy triggered by the thought of a specific stimulus. One report described a man with temporal lobe seizures induced by thinking of his childhood home.[5] Another patient with a left temporal focus on EEG had seizures when brushing his teeth but also on thinking of a toothbrush.[6] To our knowledge, there have been no reports of seizures precipitated by the thought of food or hunger alone.[1,3]

Several mechanisms have been postulated for eating epilepsy, from somatosensory and motor stimulation to gastric distension.[2,3] Primary taste areas in the anterior insula and frontal operculum are activated by taste and olfactory stimuli but also the anticipation of food.[3] Taste processing is refined in the secondary taste areas of the amygdala and orbitofrontal cortex where a greater number of neurons receive multimodal inputs.[3] Functional MRI has demon-

G Model
CLINEU-2260; No. of Pages 4
ARTICLE IN PRESS

Clinical Neurology and Neurosurgery xxx (2010) xxx–xxx

Contents lists available at ScienceDirect

Clinical Neurology and Neurosurgery

journal homepage: www.elsevier.com/locate/clineuro

Case report

Cortical propagation of Creutzfeldt–Jakob disease with codon 180 mutation

Shunsuke Kobayashi[a,*], Yuko Saito[b], Toshiyuki Maki[c], Shigeo Murayama[a,d]

[a] Department of Neurology, Division of Neuroscience, Graduate School of Medicine, University of Tokyo, 7-3-1 Hongo, Bunkyo-ku, Tokyo 113-8655, Japan
[b] Department of Pathology, National Center Hospital of Neurology and Psychiatry, 4-1-1 Ogawahigashi-cho, Kodaira, Tokyo 187-8551, Japan
[c] Maki Clinic, 131 Nishiemi, Kamogawa-shi, Chiba 299-2841, Japan
[d] Department of Neuropathology, Tokyo Metropolitan Institute of Gerontology, 35-2, Sakai-cho, Itabashi-ku, Tokyo 173-0015, Japan

ARTICLE INFO

Article history:
Received 29 June 2009
Received in revised form 28 January 2010
Accepted 13 March 2010
Available online xxx

Keywords:
CJD
Prion
Codon 180
MRI
Pathology
Immunohistochemistry
Ultrastructure
Axonal transport

ABSTRACT

A patient with Creutzfeldt–Jakob disease (CJD) with prion protein (PrP) gene codon 180 mutation (CJD 180) experienced cognitive decline over the 1.5-year period before her death. Serial magnetic resonance imaging (MRI) studies tracked stepwise propagation of cortical abnormal swelling and T2 elongations.

On postmortem examination, the cortical areas affected by CJD for relatively short periods were associated with mild spongiform changes with the number of neurons being largely preserved. The residual neurons in these areas exhibited vacuole-like dilatation of their cell body. In contrast, the atrophic cortical areas affected by CJD for long periods exhibited predominant gemistocytic astrocytosis with severe neuronal loss. The present report depicts the unique cortical propagation of CJD 180 with corresponding radiological and pathological findings. Axonal transport through corticocortical connections might underlie the disease's propagation. MRI appeared to be useful for discriminating between different pathological states and tracking the progression of CJD 180.

© 2010 Elsevier B.V. All rights reserved.

1. Introduction

Creutzfeldt–Jakob disease (CJD) usually presents with rapidly progressive dementia associated with pyramidal, extrapyramidal, and cerebellar signs. A typical radiological finding of CJD is rapid cerebral atrophy. Occasionally, lesions of CJD manifest as multifocal cortical signal abnormalities in diffusion-weighted or T2-weighted magnetic resonance imaging (MRI) [1–3]. Although several studies have suggested that abnormal magnetic resonance (MR) signals reflect spongiform changes or accumulation of prion protein (PrP) [4–6], the relationship between radiological manifestations and the pathological processes of CJD remains unclear. Here we present a CJD patient with a rare point mutation of the PrP gene at codon 180 (CJD 180). The patient presented with various neuropsychological symptoms and slowly progressive cortical abnormalities on MRI. The corresponding pathology was examined in the postmortem brain.

2. Case report

2.1. Clinical course

A 70-year-old right-handed Japanese woman was referred with a 1-month history of progressive memory loss. She did not have a particularly relevant past medical history; she had not received a blood transfusion, human growth or gonadotropin hormone treatment, dura mater transplant, corneal grafts, or undergone neurosurgical procedures. She had lived in Chiba prefecture and her family history was unremarkable. On admission, her dementia was obvious. The scores of the Mini Mental Scale and Hasegawa Dementia Scale Revised were 5/30 and 3/30, respectively. She did not show agnosia, apraxia, or neglect. Her cranial nerves and sensory motor systems were normal. Deep tendon reflexes were within normal limits and without pathological reflex. She was ambulatory and involuntary movements were not observed at that point. Routine laboratory tests were normal except for mild anemia. Results of CSF examination were normal. Protein 14-3-3 was not examined. Soon after admission, she started to show abnormal behavior such as wandering about the ward, stealing other patients' belongings, and eating her own feces. In the following 2 months, she developed fluent sensory aphasia with repetitive stereotypic speech. She also showed a tendency of excessive writing with repetitive phrases. Her neuropsychological details in this stage were reported elsewhere [7]. Within 9 months she became akinetic and mute,

* Corresponding author at: Department of Physiology, Development, and Neuroscience, University of Cambridge, Cambridge CB23DY, UK. Tel.: +44 1223 339544; fax: +44 1223 333786.
E-mail address: skoba-tky@umin.ac.jp (S. Kobayashi).

0303-8467/$ – see front matter © 2010 Elsevier B.V. All rights reserved.
doi:10.1016/j.clineuro.2010.03.015

Please cite this article in press as: Kobayashi S, et al. Cortical propagation of Creutzfeldt–Jakob disease with codon 180 mutation. Clin Neurol Neurosurg (2010), doi:10.1016/j.clineuro.2010.03.015

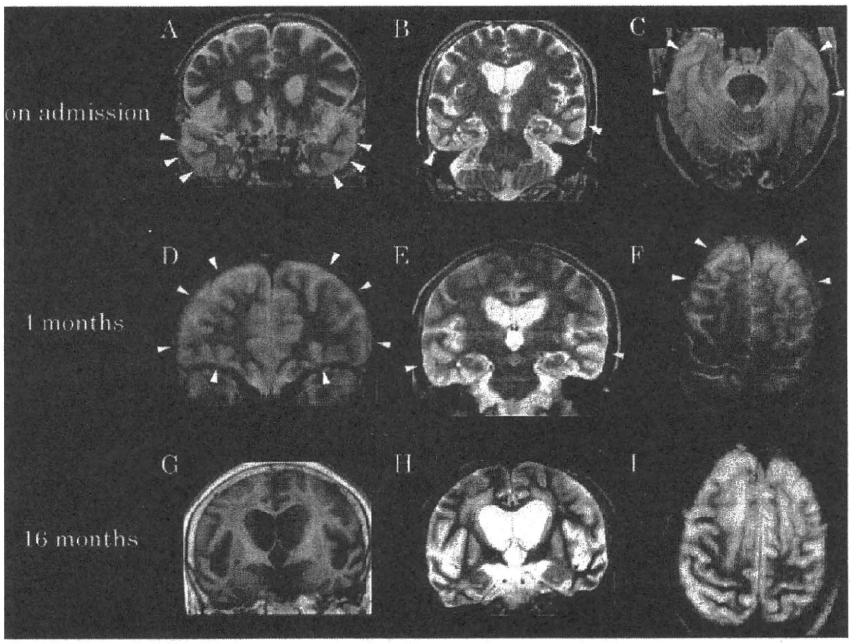

Fig. 1. Magnetic resonance images obtained on admission (A–C), and at 4 (D–F) and 16 months (G–I) after admission. Abnormal T2 elongated signals initially appeared in the temporal cortex (arrowheads in A–C) and subsequently propagated to the frontal cortex (arrowheads in D and F). After 1.5 years, the temporal cortices showed atrophy with enlarged sulci and lateral ventricles and white matter showed T2 elongated signals (G and H). At the end stage, most of the cerebral cortex showed abnormal T2 signals with relative sparing of the bilateral pre- and post-central gyri (I). All images are in T2-weighted sequence (A and B, TR 4000 TE 100; C–F, and I, TR 3500 TE 93; H, TR 4318, TE 103), except G in T1-weighted sequence (TR 600 TE 14).

and developed myoclonus in the bilateral upper limbs. Within 11 months the myoclonus became more prominent and startle responses appeared. Two years after the onset, the patient died of cholecystitis and consequent sepsis.

2.2. Radiological and encephalographic studies

Serial MRI studies revealed a stepwise progression of cortical involvement. On admission, the patient's MRI exhibited abnormal cortical thickening with T2 elongation in the bilateral temporal cortices (Fig. 1A–C). The abnormal MR signals arose in the bilateral frontal cortex and parietooccipital junction sequentially after 3 and 7 months from admission, in that order (Fig. 1D–F). One year after her admission, the frontotemporal cortices started to show atrophic changes (Fig. 1G). The cerebral cortex in the bilateral pre- and post-central gyri was relatively preserved until the patient's death (Fig. 1F and I). The cerebral white matter and basal ganglia showed T2 elongation in the end stage (Fig. 1H). The cerebellum and brainstem were spared. Diffusion-weighted imaging (DWI) was not obtained. Serial electroencephalogram studies detected gradual slowing of the basic activity along the course of the disease, which eventually became a diffuse slow wave at 3–5 Hz. However, periodic synchronous discharge (PSD) was not detected throughout the course of the disease.

2.3. Postmortem pathological studies and gene analysis

The whole brain was fixed in 10% buffered formalin. We processed blocks of the cerebrum (frontal, parietal, occipital, and temporal cortex), cerebellum, caudate, putamen, thalamus, hippocampus, and brainstem for paraffin embedding. For routine light microscopic examination, serial 6-μm-thick sections were stained with hematoxylin–eosin, Bielschowsky, and Klüver-Barrera staining. Immunohistochemistry for PrP was based on deparaffinized sections from cerebral cortex, hippocampus, caudate, putamen and thalamus, using mouse monoclonal antibody 3F4 (DAKO; 1:25) after antigen retrieval with formic acid for 3 min and autoclaving with 20 mM hydrogen chloride for 10 min. Deparaffinized hippocampal sections from a sporadic CJD case were used as control (Fig. 2J). For ultrastructural study, formalin-fixed specimens were immersed in cacodylate buffer containing 1% tannic acid overnight, postfixed in 1% osmium for 2 h, and embedded in epoxy resin. One-mm thick sections were stained with toluidine blue and appropriate areas were selected after light microscopic observation. Ultrathin sections were double stained with uranyl acetate and lead citrate.

The fixed brain weighed 950 g. Macroscopically, the frontal pole and inferior temporal cortex showed marked atrophy, but the parietal regions showed cortical swelling (Fig. 2A–C). The cerebral white matter showed myelin pallor (Fig. 2C). Microscopically, diffuse spongiform changes were observed throughout the neocortex, basal ganglia, and thalamus. The atrophic frontotemporal cortices showed gemistocytic astrocytosis with severe neuronal loss (Fig. 2D–F). The swollen part of the parietal convexity exhibited mild to moderate spongiform changes in cortical layers II–V, but the number of neurons in those areas was relatively preserved (Fig. 2G and H). Neither amyloid nor Kuru plaques were found. Some immunoreactivity to the anti-PrP antibody was detected in the temporal cortex and hippocampus (Fig. 2I), but was remarkably scarce elsewhere in the brain. Electron-microscopy studies detected membrane-bound intracellular extranuclear vacuolar inclusions in residual neurons in the examined cortical tissue, including frontal, temporal and parietal cortices (Fig. 2K). These vacuoles that occupied the cytoplasm of the neurons in the affected cortical areas were distinct from dilatation of astroglial soma and feet typically observed in so-called status spongiosus.

We analyzed PrP gene expression by extracting genomic DNA from peripheral lymphocytes by the method reported in the previous study [8]. The open reading frame of the gene was subjected to polymerase-chain-reaction direct sequencing, which revealed a

Please cite this article in press as: Kobayashi S, et al. Cortical propagation of Creutzfeldt–Jakob disease with codon 180 mutation. Clin Neurol Neurosurg (2010), doi:10.1016/j.clineuro.2010.03.015

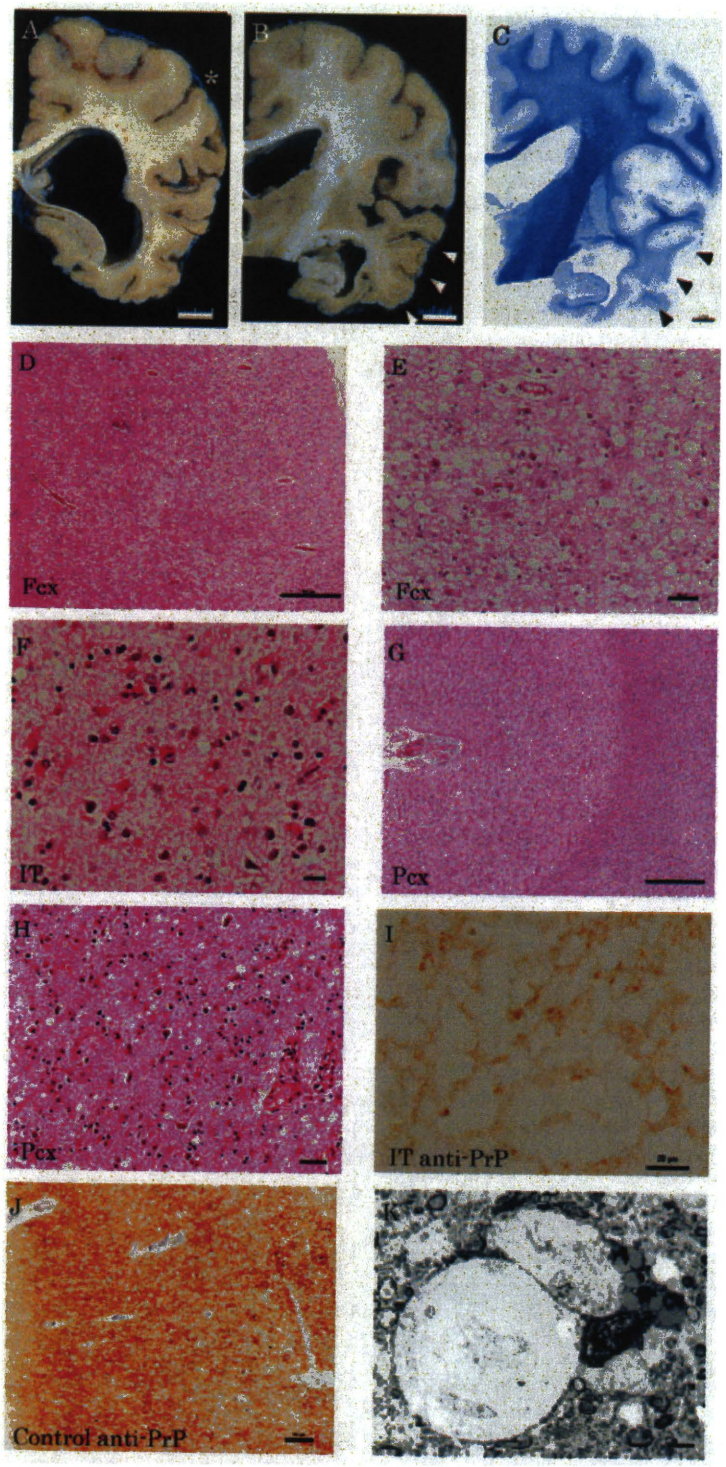

Fig. 2. Pathological findings of the postmortem brain. (A–C) A coronal macro-sections of the brain at the level of the pineal body (A) and hippocampus (B and C) (C, Klüver-Barrera staining). The temporal lobe exhibited atrophy (B and C, arrow heads), but the hippocampal formation was relatively preserved. In contrast, the parietal region appeared swollen with dense gray matter and a tight sulcal space (A, asterisk). Scale bars: A and B, 10 mm; C, 5 mm. (D–H) Representative microscopic images of gray-matter lesions (hematoxylin–eosin staining). The frontal (D and E) and temporal (F) cortices affected by CJD for long periods exhibited severe cortical atrophy with spongiform appearance. Spongiform changes were characterized by diffuse and partly confluent oval vacuoles in the neuropil in the frontal cortex (D and E). Gemistocytic astrocytosis was prominent in the temporal cortex (F). The parietal cortex, which appeared swollen macroscopically, exhibited mild spongiform changes and the number of neurons was relatively preserved (G and H). Magnification: D, G, 40× (scale bar, 500 μm); E, H, 200× (scale bar 50 μm). F, 200× (scale bar 20 μm). I: PrP immunostaining revealed perivacuolor synaptic-pattern deposits in the inferior temporal cortex (I). The immunostaining was weaker than the control with a sporadic CJD patient using the same method (J, anti-PrP antibody 3F4). Magnification: H, 400× (scale bar, 10 μm); I, 400× (scale bar, 20 μm); J, 100× (scale bar, 100 μm). K, Ultrastructure of the tissue from the parietal cortex showing spongiform changes. Scale bar, 2 μm. Fcx, frontal cortex; IT, inferior temporal cortex; Pcx, parietal cortex.

Please cite this article in press as: Kobayashi S, et al. Cortical propagation of Creutzfeldt–Jakob disease with codon 180 mutation. Clin Neurol Neurosurg (2010), doi:10.1016/j.clineuro.2010.03.015

missense PrP; GTC to ATC (Val to Ile) at codon 180. Polymorphism of codon 129 was a homozygous Met/Met.

3. Discussion

We present herein the clinical, radiological, and pathological findings of a patient with CJD 180. The present findings substantiate the previously reported unique clinical features of CJD 180 [9–15], including elderly onset, slower progression of the disease compared with sporadic CJD, lack of PSD in the electroencephalogram, and cortical swelling with T2 elongation on MRI.

The present study further elucidated a characteristic pattern of disease propagation that was observed clinically and radiologically. The temporal, frontal, and parietal cortices were involved in a stepwise manner within an interval of 3–7 months. It has been suggested that intracerebral spread of prions occurs by a domino-like reaction to a conformational change in PrP [16]. Recent research has also revealed that PrP can be transported axonally [17]. For example, experimental inoculation of prions into the mouse retina results in spongiform changes in the contralateral superior colliculus and lateral geniculate nucleus [18,19]. Thus, the abnormal MRI signals observed in the present case might reflect disease propagation through dense corticocortical connections, including the uncinate and superior longitudinal fascicles, by means of axonal transport.

The stepwise progression of the disease noted in the present case allowed us to examine the histopathology at different disease stages in the postmortem brain. The cortical swelling and T2 elongation observed in the early-stage MRI appears to correspond to cellular dilatation with vacuolar inclusions. The atrophic cortical areas observed in the chronic stage exhibited gemistocytic astrocytosis with severe neuronal loss. The areas with abnormal T2 signals did not correlate with the distribution of PrP depositions. Although MRI was clearly useful to track cortical disease progression, it may be limited in sensitivity, particularly with the T2-weighted sequence. Recent studies suggested that DWI provides higher sensitivity in detecting CJD lesions [5,20].

Masters and Richardson conducted neuropathological examination of 17 cases of CJD and found that the duration of illness correlated positively with the degree of gliosis and neuronal loss and negatively with the degree of spongiform change [21]. The present case showed a similar tendency for gliosis and neuronal loss, but spongiform changes did not decrease with advanced disease stage. The observed spongiform changes were different from those observed in status spongiosus, as they were not in pericellular or perivascular distribution [21]. The electron microscopic study was also consistent with this conclusion (Fig. 2K). Previous studies of CJD 180 also noted diffuse cortical spongiosis in advanced disease stages [12,14,22] with only one case showing replacement with tissue rarefaction (status spongiosus) [15]. Thus, persistent spongiform pathology might be characteristic to CJD 180.

Despite the use of several methods to enhance the sensitivity of the immunohistochemistry, deposition of PrP-immunoreactive material was very scarce in either the swollen or the atrophic parts of the cortex of our patient. Weak PrP immunoreactivity appears to be a common finding in CJD 180 [12–15,22]. In particular, the case of Yoshida et al. is similar to ours in that PrP deposits were found in the hippocampus, which was spared from spongiform degeneration [15]. Dissociation between spongiform changes and PrP immunoreactivity has also been reported in sporadic CJD [23] and other PrP mutations including fatal familial insomnia [24]. Thus, it leads to an important caveat in diagnosing CJD as it may manifest as severe spongiform degeneration without PrP deposits. Further investigation is required to elucidate the role of PrP in CJD pathology.

Finally, our report highlights the potential of MRI for detecting the cortical propagation of CJD. The stepwise progression of abnormal cortical MR signals might suggest the role of axonal transport in disease propagation. The new technique of diffusion tensor imaging might prove useful for the detection of any fiber-tract involvement in CJD [25].

References

[1] Gertz HJ, Henkes H, Cervos-Navarro J. Creutzfeldt–Jakob disease: correlation of MRI and neuropathologic findings. Neurology 1988;38:1481–2.
[2] Milton WJ, Atlas SW, Lavi E, Mollman JE. Magnetic resonance imaging of Creutzfeldt–Jacob disease. Ann Neurol 1991;29:438–40.
[3] Schwaninger M, Winter R, Hacke W, von Kummer R, Sommer C, Kiessling M, et al. Magnetic resonance imaging in Creutzfeldt–Jakob disease: evidence of focal involvement of the cortex. J Neurol Neurosurg Psychiatry 1997;63:408–9.
[4] Haik S, Dormont D, Faucheux BA, Marsault C, Hauw JJ. Prion protein deposits match magnetic resonance imaging signal abnormalities in Creutzfeldt–Jakob disease. Ann Neurol 2002;51:797–9.
[5] Manners DN, Parchi P, Tonon C, Capellari S, Strammiello R, Testa C, et al. Pathologic correlates of diffusion MRI changes in Creutzfeldt–Jakob disease. Neurology 2009;72:1425–31.
[6] Urbach H. Creutzfeldt–Jakob disease: analysis of the MRI signal. Neuroreport 2000;11:L5–6.
[7] Kobayashi S, Ohuchi T, Maki T. A case of probable Creutzfeldt–Jakob disease with a point mutation of prion protein gene codon 180 and atypical MRI findings. Rinsho Shinkeigaku 1997;37:671–4.
[8] Kitamoto T, Tateishi J. Human prion diseases with variant prion protein. Philos Trans R Soc Lond B Biol Sci 1994;343:391–8.
[9] Hitoshi S, Nagura H, Yamanouchi H, Kitamoto T. Double mutations at codon 180 and codon 232 of the PRNP gene in an apparently sporadic case of Creutzfeldt–Jakob disease. J Neurol Sci 1993;120:208–12.
[10] Ishida S, Sugino M, Koizumi N, Shinoda K, Ohsawa N, Ohta T, et al. Serial MRI in early Creutzfeldt–Jacob disease with a point mutation of prion protein at codon 180. Neuroradiology 1995;37:531–4.
[11] Jin K, Shiga Y, Shibuya S, Chida K, Sato Y, Konno H, et al. Clinical features of Creutzfeldt–Jakob disease with V180I mutation. Neurology 2004;62:502–5.
[12] Matsumura T, Kojima S, Kuroiwa Y, Takagi A, Unakami M, Kitamoto T. An autopsy-verified case of Creutzfeldt–Jakob disease with codon 129 polymorphism and codon 180 point mutation. Rinsho Shinkeigaku 1995;35:282–5.
[13] Shindo K, Shimokawa C, Ohta E, Inada H, Togashi S, Nitta K, et al. Autopsy-proven Creutzfeldt–Jakob disease with a codon 180 mutation showing dissociation between diffusion-weighted magnetic resonance imaging and single-photon emission computed tomography findings: is this a suggestive finding in long survival? Eur Neurol 2006;56:46–9.
[14] Suzuki K, Matsumura N, Suzuki T, Nakano H, Nagayama H, Yokoo H, et al. A case of Creutzfeldt–Jakob disease with codon 129 polymorphism and codon 180 point mutation. Nippon Ronen Igakkai Zasshi 2008;45:107–11.
[15] Yoshida H, Terada S, Ishizu H, Ikeda K, Hayabara T, Deguchi K, et al. An autopsy case of Creutzfeldt–Jakob disease with a V180I mutation of the PrP gene and Alzheimer-type pathology. Neuropathology 2009.
[16] Prusiner SB, Prions. Proc Natl Acad Sci USA 1998;95:13363–83.
[17] Butowt R, Abdelraheim S, Brown DR, von Bartheld CS. Anterograde axonal transport of the exogenous cellular isoform of prion protein in the chick visual system. Mol Cell Neurosci 2006;31:97–108.
[18] Brandner S, Raeber A, Sailer A, Blattler T, Fischer M, Weissmann C, et al. Normal host prion protein (PrPC) is required for scrapie spread within the central nervous system. Proc Natl Acad Sci USA 1996;93:13148–51.
[19] Liberski PP, Yanagihara R, Gibbs Jr CJ, Gajdusek DC. Spread of Creutzfeldt–Jakob disease virus along visual pathways after intraocular inoculation. Arch Virol 1990;111:141–7.
[20] Kallenberg K, Schulz-Schaeffer WJ, Jastrow U, Poser S, Meissner B, Tschampa HJ, et al. Creutzfeldt–Jakob disease: comparative analysis of MR imaging sequences. Am J Neuroradiol 2006;27:1459–62.
[21] Masters CL, Richardson Jr EP. Subacute spongiform encephalopathy (Creutzfeldt–Jakob disease). The nature and progression of spongiform change. Brain 1978;101:333–44.
[22] Iwasaki Y, Sone M, Kato T, Yoshida E, Indo T, Yoshida M, et al. Clinicopathological characteristics of Creutzfeldt–Jakob disease with a PrP V180I mutation and M129V polymorphism on different alleles. Rinsho Shinkeigaku 1999;39:800–6.
[23] Armstrong RA, Lantos PL, Cairns NJ. A quantitative study of the pathological changes in cortical neurons in sporadic Creutzfeldt–Jakob disease. Neuropathology 2003;23:181–7.
[24] Sasaki K, Doh-ura K, Wakisaka Y, Tomoda H, Iwaki T. Fatal familial insomnia with an unusual prion protein deposition pattern: an autopsy report with an experimental transmission study. Neuropathol Appl Neurobiol 2005;31:80–7.
[25] Fujita K, Nakane S, Harada M, Izumi Y, Kaji R. Diffusion tensor imaging in patients with Creutzfeldt–Jakob disease. J Neurol Neurosurg Psychiatry 2008;79:1304–6.

Please cite this article in press as: Kobayashi S, et al. Cortical propagation of Creutzfeldt–Jakob disease with codon 180 mutation. Clin Neurol Neurosurg (2010), doi:10.1016/j.clineuro.2010.03.015

Acta Neurol Scand 2010: 121: 127 130 DOI: 10.1111/j.1600-0404.2009.01272.x

Copyright © 2009 The Authors
Journal compilation © 2009 Blackwell Munksgaard

ACTA NEUROLOGICA
SCANDINAVICA

Clinical Commentary

Less protease-resistant PrP in a patient with sporadic CJD treated with intraventricular pentosan polysulphate

Terada T, Tsuboi Y, Obi T, Doh-ura K, Murayama S, Kitamoto T, Yamada T, Mizoguchi K. Less protease-resistant PrP in a patient with sporadic CJD treated with intraventricular pentosan polysulphate. Acta Neurol Scand: 2010: 121: 127–130.
© 2009 The Authors Journal compilation © 2009 Blackwell Munksgaard.

Treatment with intraventricular pentosan polysulphate (PPS) might be beneficial in patients with Creutzfeldt–Jakob disease. We report a 68-year-old woman with sporadic Creutzfeldt–Jakob disease who received continuous intraventricular PPS infusion (1–120 μg/kg/day) for 17 months starting 10 months after the onset of clinical symptoms. Treatment with PPS was well tolerated but was associated with a minor, transient intraventricular hemorrhage and a non-progressive collection of subdural fluid. The patient's overall survival time was well above the mean time expected for the illness but still within the normal range. Post-mortem examination revealed that the level of abnormal protease-resistant prion protein in the brain was markedly decreased compared with levels in brains without PPS treatment. These findings suggest that intraventricular PPS infusion might modify the accumulation of abnormal prion proteins in the brains of patients with sporadic Creutzfeldt–Jakob disease.

T. Terada[1], Y. Tsuboi[2], T. Obi[1], K. Doh-ura[3], S. Murayama[4], T. Kitamoto[5], T. Yamada[2], K. Mizoguchi[1]

[1]Department of Neurology, Shizuoka Institute of Epilepsy and Neurological Disorders, Shizuoka, Japan; [2]Department of Neurology, Fukuoka University School of Medicine, Fukuoka, Japan; [3]Division of Prion Biology, Department of Prion Research, Tohoku University Graduate School of Medicine, Sendai, Japan; [4]Department of Neuropathology, Tokyo Metropolitan Institute of Gerontology, Tokyo, Japan; [5]Department of Neurological Science, Tohoku University Graduate School of Medicine, Sendai, Japan

Key words: Creutzfeldt–Jakob disease; intraventricular infusion; pentosan polysulphate; prion protein

Tomokazu Obi, Department of Neurology, Shizuoka Institute of Epilepsy and Neurological Disorders, Urushiyama 886, Aoi-ku, Shizuoka 420-8688, Japan
Tel.: +81 54 245 5446
Fax: +81 54 247 9781
e-mail: obit@szec.hosp.go.jp

Accepted for publication September 3, 2009

Introduction

Current options for the treatment of Creutzfeldt–Jakob disease (CJD) do not slow or halt disease progression. Treatment with pentosan polysulphate (PPS), a large polyglycoside molecule with anti-thrombotic and anti-inflammatory properties, administered intraventricularly to bypass the blood brain barrier can both prolong the survival period and reduce the extent of abnormal prion protein (PrP) deposition in the brains of rodent prion disease models (1). The safety and efficacy of intraventricular PPS treatment in humans with CJD, however, remains largely unknown (2–6). We report a patient with sporadic CJD (sCJD) treated with continuous intraventricular PPS administration starting 10 months after the onset of clinical symptoms.

Case report

The patient was a 68-year-old woman with neither a family history of prion disease nor previous history of neurological disease. She had never received cadaveric growth hormone injection, a dura mater transplant, or a cornea transplant. She noticed unsteadiness of gait and forgetfulness at the age of 65 years. One month later, unsteadiness and intellectual deterioration progressed and myoclonic jerks appeared. Cerebrospinal fluid analysis was normal except for an increased concentration of neuron-specific enolase (66 ng/ml, normal < 25) and the presence of 14-3-3 protein. EEGs showed periodic spike/slow–wave complexes (spike–wave complexes). Diffusion-weighted MRI showed abnormal high-intensity signals in the head of the caudate nucleus, putamen and insular cortex.

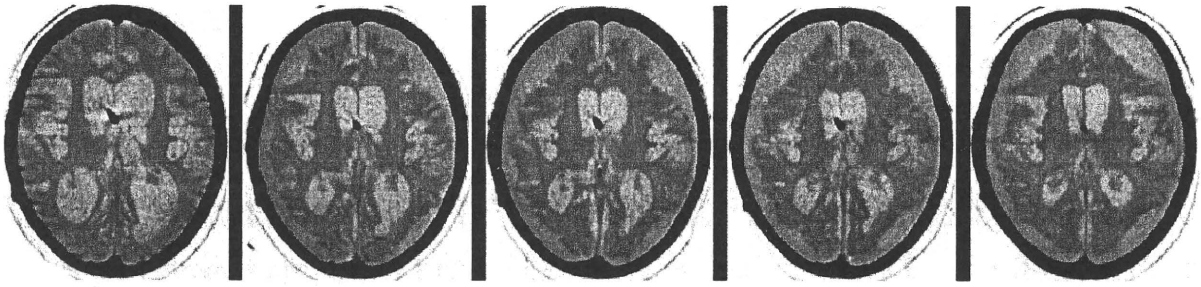

Figure 1. Sequential follow-up CT scans from 12 to 17 months after start of intraventricular PPS infusion. (A) Non-enhanced CT scan 12 months after start of intraventricular PPS infusion. Note the severe cortical and subcortical atrophy with enlargement of ventricular system. (B) Non-enhanced CT scan 13 months after start of intraventricular PPS infusion. Note the subdural fluid collection and the small sedimentation of blood in the left posterior horn. (C, D, E) Non-enhanced CT scan 14, 15, 17 months after start of intraventricular PPS infusion, respectively. The blood sedimentation in the posterior horn disappeared next month and subdural fluid collections were not progressing. No intraventricular hemorrhage was noted in scan E which was taken 7 days before death.

Genetic analysis of the *PrP* gene revealed methionine homozygosity at codon 129 and no mutations. The patient continued to deteriorate and became doubly incontinent, bed-bound and mute. Five months after the onset of symptoms, she developed akinetic mutism. Seven months after onset, the myoclonic jerks and spike–wave complexes disappeared. Ten months after onset, treatment with intraventricular PPS administration commenced under signed informed consent from her family. She received implantation of a right ventricular catheter and an epigastric subcutaneous drug infusion pump (Archimedes; 20-ml reservoir, flow rate 0.5 ml/24 h; Codman & Shurtleff Inc, Raynham, MA, USA). Using a reported protocol (5), infusion of intraventricular PPS (SP 54; bene-Arzneimittel GmbH, Munich, Germany) was started at 1 μg/kg/day, with subsequent escalation to the dose of 60 μg/kg/day 7 months later, and to the target dose of 120 μg/kg/day 15 months later, which continued until she died. However, her clinical condition did not improve and she still displayed akinetic mutism. A series of brain CT examinations demonstrated progressive brain atrophy, a transient intraventricular minor hemorrhage at the time of 13 months later, and a non-progressive collection of subdural fluid until 7 days before death (Fig. 1). Her clinical condition did not deteriorate from the time of 12 to 16 months. Monthly blood cell counts and coagulation measurements were normal. Twenty-seven months after onset, at age 68 years, the patient died of pneumonia which occurred 11 days before death and was aggravated.

Methods

Autopsy was performed within 2 h after death. The right temporal pole of the brain was dissected out and stored at −70°C. The other parts of the brain were fixed in neutral buffered formalin. Sections of representative areas of the brain were stained with hematoxylin–eosin, Klüver–Barrera and immunohistochemical methods.

Immunohistochemical staining

The following primary antibodies were used: anti-phosphorylated α-synuclein (monoclonal; Wako, Osaka, Japan), anti-phosphorylated tau (AT8, monoclonal; Fitzgerald, Concord, MA, USA), anti-amyloid β 1–42 (polyclonal; IBL, Takasaki, Japan) and anti-PrP (3F4, monoclonal; Signet, Dedham, MA, USA).

Prion protein analysis

Protease-resistant PrP was extracted from cerebral tissues of this and other sCJD patients as previously described (7). Samples were subjected to 13.5% SDS-PAGE and transferred to polyvinylidene fluoride membrane. 3F4 antibody was used as the primary antibody. Anti-mouse EnVision (Dako, Glostrup, Denmark) was used as the secondary antibody. Enhanced chemiluminescence detection (Amersham Bioscience, Little Chalfont, UK) was used to visualize Western blots. The signal intensities of the blots were quantified with Quantity One software using an imaging device, Vasa Doc 5000 (Bio-Rad Laboratories, Hercules, CA, USA) (7).

For quantitative comparison of protease-resistant PrP levels, we initially analyzed 10-fold diluted samples derived from 0.5 mg wet-weight brain tissue from the temporal pole to identify suitable dilutions. For controls, we included frontal lobe tissues from three sCJD patients (all homozygous for methionine at codon 129 of the *PrP* gene) not treated with intraventricular PPS infusion: two with a type 1 pattern of protease-resistant PrP signals in Western blot analysis (sCJD MM1) whose brains were uniformly, severely atrophied similarly to the

patient's brain, and one with cortical-type sCJD and a type 2 pattern (sCJD MM2C).

Results

Post-mortem neuropathology

The unfixed brain weighed 660 g and showed walnut-shaped severe atrophy. A massive intraventricular hematoma was present. The shape of blood cells in the hematoma was completely preserved, with no infiltration by reactive cells such as macrophages and glial cells. The PPS infusion catheter had been correctly inserted into the right lateral ventricle, and the source of hemorrhage could not be identified. There was extensive, symmetrical cortical atrophy, but the hippocampi were relatively spared.

Microscopy demonstrated extensive neuronal loss and spongiosis in most areas of the cerebral cortices, with collapsed cytoarchitecture. Axonal loss with secondary myelin loss was present in the central white matter, accompanied by a cellular reaction containing both astrocytes and microglial cells throughout the areas of myelin damage. There was widespread gliosis in the basal ganglia, thalami and cerebellar molecular layer. The cerebellar granular layer showed marked neuronal loss with gliosis and axonal loss, accompanied by secondary myelin loss in the cerebellar white matter. Lewy bodies, amyloid plaques and neurofibrillary tangles were not observed. PrP staining showed a widespread synaptic pattern in the cerebral cortices, basal ganglia and thalami. Synaptic staining was also present in the molecular layer of the cerebellum, with intense coarse deposits in the granular layer. No plaque-like PrP deposits were identified in any brain regions. The findings were consistent with the diagnosis of sCJD. There was no laterality in the extent of the neuronal loss, spongiosis, gliosis or synaptic PrP deposition.

Prion protein analysis

Western blot analysis of protease-resistant PrP showed a type 1 pattern (Fig. 2) identical to those of the two classical sCJD MM1 cases. Protease-resistant PrP levels were 1/3 to 1/8 of those in the sCJD patients with no intraventricular PPS treatment.

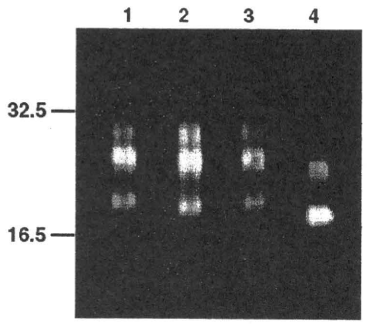

Figure 2. Comparative Western blot analysis of protease-resistant PrP. Protease-resistant PrP is categorized into three types based on the pattern of glycoform and mobility of PrP bands in Western blot analysis. Protease-resistant PrP, type 1, from the brain of this patient (threefold-diluted, lane 2) and three control subjects with sCJD: lane 1, 30-fold-diluted brain sample from an sCJD MM1 subject (65-year-old woman with a survival time of 11 months); lane 3, 20-fold-diluted brain sample from another sCJD MM1 subject (74-year-old woman with a survival time of 16 months); and lane 4, 40-fold-diluted brain sample from an sCJD MM2C subject. An unglycosylated PrP band from this patient (lane 2, arrowhead) mapped slightly lower than those in the other sCJD MM1 subjects (lanes 1 and 3). We normalized signal intensity to the band in lane 2 ($100/mm^2$). After dilution powers were also considered, the corrected signal intensities for lanes 1, 3 and 4 were $680/mm^2$, $300/mm^2$ and $770/mm^2$, respectively.

Discussion

Here, we present a patient with sCJD who was treated with intraventricular PPS for 17 months. The PPS dose of 120 μg/kg/day was well tolerated but was associated with a minor, transient intraventricular hemorrhage and collection of subdural fluid. A fresh intraventricular hematoma found during autopsy probably occurred at the agonal stage, because blood cell shape was preserved and there was no inflammatory cell infiltration. Moreover, this intraventricular hematoma is unlikely to alter the patient's clinical course, because pneumonia which occurred 11 days before death was rapidly aggravated to respiratory failure responsible for her death, and no intraventricular hemorrhage was detected on CT scan 7 days before death.

Pentosan polysulphate is a candidate anti-prion compound that has shown efficacy in animal models (1, 8, 9), and has been administered by intraventricular infusion in several patients (2–6). Thrombocytopenia and abnormal coagulation can occur occasionally with PPS but did not occur in our patient. A minor, transient intraventricular hemorrhage and a non-progressive collection of subdural fluid appeared during PPS treatment but did not influence clinical progression. These findings may have resulted from a pressure imbalance within the intraventricular or subdural spaces caused by PPS infusion, although this speculation requires further proof. Overall, a PPS dose of 120 μg/kg/day seems well-tolerated and does not cause major adverse effects in CJD patients (2–6).